Batch culture and species effects modulate the decoupling between diatom frustule-bound and biomass nitrogen isotope signatures

Jochem Baan[1]*, Moritz F. Lehmann[1], Ansgar Kahmen[2], Anja S. Studer[1]

[1]University of Basel, Department of Environmental Sciences, Bernoullistrasse 30, 4056 Basel, Switzerland

[2]University of Basel, Department of Environmental Sciences - Botany, Schönbeinstrasse 6, 4056 Basel, Switzerland

*Corresponding author e-mail: jochem.baan@unibas.ch

Abstract

The stable nitrogen (N) isotope composition of organic matter encapsulated in diatom silica frustules ($\delta^{15}N_{DB}$) from sedimentary records has been used as a proxy for reconstructing N consumption dynamics in the ocean over geologic time scales. This proxy relies on the assumption that $\delta^{15}N_{DB}$ tracks biomass $\delta^{15}N$, without being affected by internal N-isotope fractionation. However, recent ground-truthing efforts have shown that $\delta^{15}N_{DB}$ can diverge from biomass $\delta^{15}N$ values, though the extent and mechanisms behind this decoupling remain unclear.

In this study, we cultured two freshwater and two marine diatom species in batch cultures to test whether $\delta^{15}N_{DB}$ (1) is subject to species-dependent internal ^{15}N fractionation, and (2) reflects the $\delta^{15}N$ of source nitrate to the same extent as biomass $\delta^{15}N$ values, assessing asynchronous integration of the N isotope signal. We monitored the N isotope systematics during diatom growth by measuring $\delta^{15}N$ values in nitrate, bulk biomass and frustule-bound organic N throughout batch culture progression. We found that $\delta^{15}N_{DB}$ did not follow typical Rayleigh fractionation dynamics and remained relatively stable, while biomass $\delta^{15}N$ increased predictably with progressive fractional nitrate consumption. The observed divergence could not be explained by de-synchronized integration of source-nitrate $\delta^{15}N$ values into biomass versus frustule-bound organic N (i.e. delayed incorporation into frustule-bound material), as newly formed frustules clearly recorded the $\delta^{15}N$ of the ^{15}N-labeled nitrate added during growth. This confirmed that $\delta^{15}N_{DB}$ values capture the isotopic signature of newly assimilated nitrate rather than N derived from internal or legacy pools. We hypothesize that shifts in growth conditions during batch culture progression altered the interaction between carbon and nitrogen metabolism, leading to physiologically driven variation in internal ^{15}N fractionation and corresponding offsets between

$\delta^{15}N_{DB}$ and biomass $\delta^{15}N$. Such sensitivity to internal isotope fractionation during biosynthesis has important implications for the interpretation of sedimentary $\delta^{15}N_{DB}$ records.

Introduction

The nitrogen (N) isotopic composition ($\delta^{15}N$) of diatom frustule-bound organic matter ($\delta^{15}N_{DB}$) from sedimentary archives has been used as a promising proxy indicator for reconstructing nitrate utilization across various timescales in the ocean (Sigman *et al.*, 1999; Robinson *et al.*, 2004; Studer *et al.*, 2015; Ai *et al.*, 2020), and more recently, in lacustrine environments for paleoenvironmental reconstructions (Studer *et al.*, 2024). The main advantage of this proxy is that $\delta^{15}N_{DB}$ is thought to be physically protected from diagenetic alteration and bacterial degradation, unlike the $\delta^{15}N$ values of organic matter in bulk sediment which are known to be susceptible to post-depositional alterations (Lehmann *et al.*, 2002; Robinson *et al.*, 2012). Despite the fact that the $\delta^{15}N_{DB}$ proxy has been applied in palaeoceanographic research for more than two decades, the mechanisms by which the $\delta^{15}N$ signature of assimilated inorganic N is transferred into diatom biomass, and ultimately preserved in $\delta^{15}N_{DB}$, remain poorly understood.

When diatoms grow, their cell walls become silicified, forming opaline frustule structures. This silicification occurs after mitosis, through the synthesis of new valves, and during cell expansion, when girdle bands are formed (Kröger & Poulsen, 2008). Frustule formation is facilitated by several N-containing organic compounds (e.g. silaffins, silacidins, and polyamines), which act as organic templates for silicate precipitation (Poulsen *et al.*, 2003; Bridoux & Ingalls, 2010; Richthammer *et al.*, 2011). These compounds become encapsulated within the frustule and can persist over long-time scales. The N in these frustule-bound organic compounds originates from the intracellular organic N pool in the diatom, which in turn derived from the assimilation of inorganic N in the surrounding water. Under this framework, the $\delta^{15}N$ values of assimilated inorganic N should be transferred into, and reflected by, cellular organic N, and thus into $\delta^{15}N_{DB}$ values. Accordingly, $\delta^{15}N_{DB}$ values have been interpreted as proxies for nitrate

consumption/utilization (Robinson *et al.*, 2005; Brunelle *et al.*, 2007), nitrogen cycling in general (Kalansky *et al.*, 2011), and N eutrophication (Studer *et al.*, 2024).

Efforts to ground-truth the diatom frustule-bound $\delta^{15}N$ paleo-proxy through controlled batch culture experiments have shown that $\delta^{15}N_{DB}$ values can differ substantially from biomass $\delta^{15}N$ values (Horn *et al.*, 2011; Jones *et al.*, 2022; Robinson *et al.*, 2025). Horn *et al.*, (2011) found $\delta^{15}N_{DB}$ values lower than those of biomass, with species-specific offsets, whereas Jones *et al.*, (2022) found the opposite pattern. More recently, Robinson *et al.*, (2025) observed both positive and negative offsets, depending on species, and suggested that the nitrate-to-silicate uptake ratio may play a modulating role. Overall, these findings suggest that $\delta^{15}N_{DB}$ values can vary substantially and do not consistently track biomass $\delta^{15}N$ values, and that the underlying drivers of the offset are still poorly understood.

Culturing diatoms under controlled environmental conditions enables detailed observation of N isotope transfer from source nitrate into diatom biomass and frustule-bound material. In batch cultures, the $\delta^{15}N$ values of nitrate and accumulated biomass typically follow Rayleigh-type substrate-product dynamics (Mariotti *et al.*, 1981; Waser *et al.*, 1998). Once assimilated, N is processed into various proteins and other N-containing biomolecules, including those found in diatom frustules (Sumper & Brunner, 2008; Kröger & Poulsen, 2008; Bridoux & Ingalls, 2010; Richthammer *et al.*, 2011; Kirkham *et al.*, 2017). As diatoms synthesize frustules over the course of a batch culture, the frustule-bound organic N pool accumulates. It might therefore be expected that $\delta^{15}N_{DB}$ values reflect the integrated isotopic composition of the accumulating frustule-bound organic matter similar to the integrated $\delta^{15}N$ signal in bulk biomass (Mariotti *et al.*, 1981). However, this expectation rests on two key assumptions: (1) that ^{15}N fractionation associated with the synthesis of frustule-bound organic compounds is constant, and (2) that the integration time

window of the isotope signal incorporation from the inorganic N source is the same for biomass and frustule-bound organic N. With regards to the first assumption, internal N-isotope fractionation during biosynthesis may vary due to metabolism-driven biochemical reactions (Werner & Schmidt, 2002; Tcherkez & Hodges, 2008). Additionally, the $\delta^{15}N$ values of amino acids (the building blocks of proteins and polyamines) can vary between compounds and across species (Macko *et al.*, 1987; Werner & Schmidt, 2002), suggesting that $\delta^{15}N_{DB}$ values may also depend on (species-specific) differences in the frustule-bound organic N matrix/composition (Sumper & Brunner, 2008; Bridoux & Ingalls, 2010). As for the second assumption, frustule-bound organic N may derive from an internal N pool with a distinct isotopic signature, potentially leading to asynchronous $\delta^{15}N$-signal integration relative to bulk biomass. To date, neither of these assumptions have been experimentally verified, yet the observation that $\delta^{15}N_{DB}$ values can be both higher and lower than biomass $\delta^{15}N$ values (Horn *et al.*, 2011; Jones *et al.*, 2022; Robinson *et al.*, 2025) implies that at least one of them may not hold. As such, it remains uncertain whether $\delta^{15}N_{DB}$ values consistently reflect biomass and/or nitrate $\delta^{15}N$ values and thus exhibit predictable Rayleigh-type fractionation behavior.

Diatom culture studies aimed at ground-truthing the $\delta^{15}N_{DB}$ proxy have so far exclusively focused on marine species. However, since the proxy has recently also been applied in lacustrine systems (Studer *et al.*, 2024), it is important to investigate the relationship between nitrate, biomass and frustule-bound $\delta^{15}N$ values in freshwater diatoms. Moreover, freshwater species generally exhibit higher silicate uptake rates compared to most marine species (Conley *et al.*, 1989). Therefore, further insight into whether, and how, silicate-to-nitrate uptake ratios influence $\delta^{15}N_{DB}$ values relative to biomass (Robinson *et al.*, 2025) can be achieved by including freshwater taxa in the experimental design.

In this study, we cultured two marine and two freshwater diatom species under controlled environmental conditions, with nitrate as the limiting nutrient. These batch cultures were closely monitored, and $\delta^{15}N$ values of nitrate, bulk biomass and frustule-bound organic N were monitored throughout the progression of each culture. This experimental setup allowed us to specifically test whether variation in frustule-bound $\delta^{15}N$ could be explained by that of nitrate and/or biomass, and whether the observed patterns were consistent (1) among species, (2) between ecosystems (freshwater vs. marine), and (3) over time during batch culture progression. In a separate ^{15}N-labeling experiment we manipulated the $\delta^{15}N$ of the nitrate source during growth, to assess if bulk-biomass and frustule-bound $\delta^{15}N$ values capture the nitrate isotope signal concurrently, or whether differences in isotopic integration timing exist between these N pools. Overall, our results highlight that $\delta^{15}N_{DB}$ values do not strictly follow Rayleigh-type dynamics in batch culture. However, this deviation from expected patterns is not due to (species-specific) differences in the timing of nitrate $\delta^{15}N$ incorporation into diatom biomass versus frustule-bound N. Instead, our findings suggest that the observed offset is more likely driven by variable, growth condition-dependent biochemical ^{15}N fractionation.

Materials and Methods

Diatom cultures

Two colony-forming freshwater species were selected: the centric *Aulacoseira granulata* and the pennate *Fragilaria capucina*, both isolated from Swiss lakes and kindly provided by Marta Reyes (Swiss Federal Institute for Aquatic Research, Dubendorf, Switzerland). Two marine diatom species forming individual cells were obtained from the Culture Collection of Algae & Protozoa (CCAP, Scottish Association for Marine Science, Dunbeg, Scotland, United Kingdom): *Chaetoceros calcitrans* (CCAP 1085/3), a small centric diatom, and *Coscinodiscus radiatus* (CCAP 1013/11), a large centric diatom.

The growth medium for freshwater diatoms was based on the CCAP 'Diatom Medium' recipe, with some modifications, resulting in the following starting concentrations: 102 µM $Ca(NO_3)_2$, 100 µM K_2HPO_4, 101 µM $MgSO_4$, 200 µM $KHCO_3$, 200-350 µM Na_2SiO_3, 36 µM Fe-EDTA, 5 µM $MnCl_2$, 0.2 µM $CuSO_4$, 0.9 µM $ZnSO_4$, 0.5 µM Na_2MoO_4, 40 µM H_3BO_3, and vitamins (0.04 mg/L cyanocobalamin, thiamine HCl, and biotin each).

The medium for marine diatoms was based on the ESAW artificial seawater recipe (Harrison *et al.*, 1980; Berges *et al.*, 2001), with some modifications. The base seawater composition followed ESAW with the exception that NaBr was used instead of KBr. Micronutrient composition also followed ESAW, except $CoSO_4$ was replaced with CoCl. Since copper is not typically included in ESAW, but was added to the freshwater medium, 0.1 µM of $CuSO_4$ was also added here. Iron was provided as 36 µM Fe-EDTA. The same vitamin concentrations were used as in the freshwater medium. Lastly, nitrate, phosphate and silicate were added at starting concentrations of 254 µM $Ca(NO_3)_2$, 103 µM K_2HPO_4 and 150-350 µM Na_2SiO_3. In order to

obtain sufficient frustule material from *C. calcitrans*, which is weakly silicifying, a higher initial nitrate concentration (~508 μM) was used. The pH of the artificial seawater medium was adjusted to 8.1 ± 0.1 using a 0.5 M NaOH prior to filtration.

All media were filter-sterilized using sterile 0.2 μm polyether sulfone (PES) membranes into autoclaved containers. Since the Na_2SiO_3 stock solution had a high pH (12-13), its addition influenced the pH of the medium and caused precipitation and filtration problems. Therefore, silicate was added aseptically *after* filtration. In some freshwater batch cultures (Table 1), 400 mg/L N-Tris(hydroxymethyl)methyl-2-aminoethanesulphonic acid (TES) buffer was added to stabilize pH during growth, and to counteract the pH rise from Na_2SiO_3 addition. For marine cultures and freshwater batch cultures 5 & 6 (Table 1), silicate was added as a neutralized colloid: a 50 mM Na_2SiO_3 stock solution was titrated with 1M HCl to pH 7.5-8.5 while stirring, forming a Na_2SiO_3 colloid that was then aseptically added post-filtration.

Diatom culture stocks were maintained in 100-200 mL Erlenmeyer flasks, filled with 50-100 mL of medium and covered with aluminum foil. Cultures were grown at 20 °C under a 12h/12h light/dark cycle with ~140 μmol m^{-2} s^{-1} photons from LED lighting in the growth chambers (MLR-350, SANYO, Japan). Stocks were manually stirred daily, and refreshed every 2-4 weeks, either by addition of medium, or by transferring 5 mL of culture into fresh 50 mL medium in a new flask.

The batch culture experiments were conducted in 20-L clear polycarbonate carboys filled with sterile-filtered medium. Each carboy was fitted with three ports: one for sampling, one for air inflow to aerate the medium, and one for air outflow. Air was supplied via a compressed air system through 0.2 μm hydrophobic PTFE filters. Carboys were placed in a large custom-built walk-in phytotron chamber at 20 °C, with ceiling-mounted LEDs providing ~140 μmol m^{-2} s^{-1} photons. A

12h/12h light/dark cycle was used, with gradual light-intensity ramp-up and ramp-down over the first and last hour of the light period, respectively. Carboys were equilibrated with ambient air for at least 24 h prior to inoculation. Cultures were inoculated with 20-40 mL of recently transferred stock culture. This relatively small inoculum delayed biomass sample collection in early incubation stages but minimized disruption of expected closed-system isotope dynamics. Each species was cultured in at least two replicate batch cultures.

Media were regularly sampled to monitor growth, pH, and nutrient (i.e., nitrate and silicate) consumption. Growth was tracked via *in vivo* fluorescence using an AquaFluor handheld fluorometer (Turner Designs, CA, USA). Samples were filtered through 0.22 μm PES syringe filters. In freshwater cultures, nitrate concentrations were measured by spectrophotometric analysis using LCK339 nitrate test kits (Hach, Germany). In artificial seawater, nitrate was measured using a chemiluminescence method (described below) due to interference from high ion concentrations with the nitrate test. For silica analysis, filtered samples were acidified to ~pH 2 using 1 μL 6N HCl per mL of sample. Silicate concentrations were determined photometrically (Strickland & Parsons, 1972), using molybdate-3, citric acid, and amino acid F reagents, and calibrated against a 1 mg/l SiO_2 standard (Hach, Germany). When silicate became limiting before a substantial nitrate fraction was consumed, additional silicate was added to the batch culture. Samples for nitrate concentration and $\delta^{15}N$ analysis were stored frozen at -20 °C. Silicate samples were stored at room temperature to avoid polymerization at high silicate concentrations.

Once biomass reached sufficient density, 1-4L samples were harvested at regular time intervals. Biomass was concentrated by centrifugation and split into two aliquots: one for bulk biomass $\delta^{15}N$ and $\delta^{13}C$ measurements and elemental (N and C) analysis, and one for the analysis of frustule-bound $\delta^{15}N$ values. Bulk biomass aliquots were frozen at -20 °C, freeze-dried, and

stored in the dark at room temperature prior to analysis. Frustule-bound $\delta^{15}N$ samples were stored frozen at -20 °C until further processing.

Two replicate batch-cultures of each freshwater diatom species (culture numbers 5 & 6; Table 1) were grown as described above, except that after the first 2-4 biomass samples had been harvested, and once nitrate had decreased to ~50 % of its initial concentration, a 4 mM solution of ^{15}N-labelled nitrate ($\delta^{15}N \approx 4000$ ‰) was added. The volume added was calculated based on mass-balance targeting an 80-100 ‰ increase in nitrate $\delta^{15}N$, with minimal change in nitrate concentration (1-2 μM). After the ^{15}N-nitrate spike, cultures were monitored and harvested regularly until all nitrate was consumed. In this experiment, the relative abundance of empty frustules in harvested biomass was assessed microscopically to determine whether a potential decoupling between biomass and frustule-bound $\delta^{15}N$ value could result from an increased contribution of older, unlabeled frustules.

Sample processing and isotope analysis

Nitrate concentration measurements

Nitrate concentrations were determined using a chemiluminescence method. Briefly, samples were injected into a heated 0.1 M vanadium(III) in 2N HCl solution to convert sample nitrate to NO (Braman & Hendrix, 1989), followed by chemiluminescent detection of the NO gas after reaction with ozone in a TELEDYNE T200 $NO/NO_2/NOx$ analyzer (TELEDYNE API, CA, USA). Sample nitrate concentrations were determined by comparison to multiple injections of KNO_3 reference standards of known nitrate concentrations.

Biomass $\delta^{15}N$ and $\delta^{13}C$ values, and N and C content

Aliquots of 1-3 mg of freeze-dried diatom biomass were weighed into tin cups. Biomass $\delta^{15}N$ and $\delta^{13}C$ values, as well as total N and C contents were determined using a Delta V Plus isotope ratio mass spectrometer (IRMS; Thermo Fisher Scientific) coupled to a Flash Elemental Analyzer (EA). Scale normalization for $\delta^{15}N$ values was performed using USGS61 ($\delta^{15}N$ = -2.87 ‰; $\delta^{13}C$ = -35.05 ‰), and USGS62 ($\delta^{15}N$ = 20.17 ‰; $\delta^{13}C$ = -14.79 ‰) international reference materials. For samples from the ^{15}N-labeled nitrate addition experiments, we also additionally included USGS41 ($\delta^{15}N$ = 47.57 ‰; $\delta^{13}C$ = 37.63 ‰). Scale normalization for $\delta^{13}C$ values was based on USGS40 ($\delta^{15}N$ = -4.52 ‰; $\delta^{13}C$ = -26.39 ‰), USGS62, and USGS64 ($\delta^{15}N$ = 1.76 ‰; $\delta^{13}C$ = -40.81 ‰) standards. Elemental N and C contents were determined from IRMS peak areas using a calibration curve that was established based on the analysis of a wheat flour standard (1.36 % N; 39.38 % C; Säntis analytical, Switzerland) and EDTA (9.58 % N; 41.06 % C). Analytical reproducibility was assessed by repeated analysis (n = 5) of biomass from a commercial diatom culture (*Thalassiosira weissflogii*, TW1800, Reed Mariculture, CA, USA), yielding mean ± SD $\delta^{15}N$ and $\delta^{13}C$ values of 6.9 ± 0.3 ‰ and -10.50 ± 0.1 ‰, respectively.

Frustule-bound and ambient nitrate $\delta^{15}N$ analysis

All glassware used in frustule-bound $\delta^{15}N$ analysis was cleaned by combustion in a muffle oven at 450 °C for 6 h. Diatom frustules were cleaned as described by (Morales *et al.*, 2013). Briefly, diatom samples underwent at least two cycles of sonication in a 2 % (w/v) sodium dodecyl sulfate (SDS), followed by centrifugation, decanting, sonication in purified water, centrifugation and decanting. Non-frustule-bound biomass was then further removed through subsequent steps of oxidation by sulfuric acid and potassium permanganate ($KMnO_4$), 14 % perchloric acid for 1 h at 100 °C, and 70 % perchloric acid for 1 h at 100 °C. Cleaned diatom frustules were collected on

2 µm polycarbonate filter membranes and rinsed thoroughly with purified water. Diatom samples were then dried at 60 °C in a dedicated, low-N oven. Dissolution of the opal frustules and oxidation of the released frustule-bound organic N was performed within one week of drying.

Approximately 2-7 mg of dried frustules were weighed into 4 mL glass vials (smaller samples were transferred using purified water). Persulfate oxidizing reagent (POR) solution used to dissolve diatom frustules and oxidize organic N to nitrate was added (1.5ml per vial). POR consisted of potassium persulfate (5% w/v) and sodium hydroxide (5% w/v). The potassium persulfate salt was pre-purified to remove residual N via multiple dissolution and crystallization cycles. Vials were autoclaved for 90 minutes at 121 °C. Following oxidation, sample pH was adjusted to 4 - 7 using ultrapure HCl. Nitrate concentrations of oxidized frustule samples were determined using the chemiluminescence method described above and $\delta^{15}N$ was measured using the denitrifier method (see below; Sigman *et al.*, 2001). Each sample batch included vials with known concentrations of amino acid standards (USGS64, USGS65, USGS40 and USGS41) and procedural blanks to assess recovery, oxidation completeness, and blank contribution. Procedural blank size and $\delta^{15}N$ values were used for post-correction of frustule-bound $\delta^{15}N$ values using isotope mass-balance considerations. Consistency of the frustule-cleaning and oxidation method was assessed by routinely including material from a commercial diatom culture of *T. weissflogii* (TW1800, Reed Mariculture). This regularly co-processed material yielded $\delta^{15}N$ values of 0.4 ± 0.3 ‰ (n = 10). As additional quality control, cleaned diatom frustule material, from two reference sources - a commercial *Thalassiosira pseudonana* culture (TP1800, Reed Mariculture) and a phytoplankton sample collected in Lake Murten, Switzerland (2023) - was cleaned once in bulk, stored in sealed vials isolated from the atmosphere, and regularly co-analyzed across runs. These samples yielded frustule-bound $\delta^{15}N$ values of -6.1 ± 0.5 ‰ (n = 9), and 8.4 ± 0.4 ‰ (n = 8),

respectively. Across all diatom culture samples, the mean procedural blank contribution was 1.5 %, with a maximum of 5.6 %. Corresponding corrections to frustule-bound $\delta^{15}N$ values were, on average, 0.13 ‰ with a maximum of 0.63 ‰ $\delta^{15}N$.

Ten nanomoles of dissolved nitrate (from culture medium or from oxidized diatom frustules) was converted to N_2O using the denitrifier method (Sigman *et al.*, 2001). The $\delta^{15}N$ of the resulting N_2O was measured by gas-chromatography isotope ratio mass spectrometry (Thermo Delta V Plus GC-IRMS, Thermo Fisher Scientific) coupled to a Gasbench used for N_2O concentration and purification. Scale normalization was performed using nitrate reference materials with known $\delta^{15}N$: USGS34 (-1.8 ‰), IAEA N3 (4.7 ‰) and a lab-internal standard UBN-1 (14.15 ‰). For the analysis of nitrate samples ^{15}N-labelling experiment, the USGS32 standard ($\delta^{15}N$ = 180 ‰) was also included. Analytical precision was assessed through repeated analyses of nitrate from a Deep-Pacific-Ocean water sample (5.2 ± 0.1 ‰, n = 28).

Data analysis

All $\delta^{15}N$ values are reported relative to AIR-N_2, and $\delta^{13}C$ values relative to the Vienna Pee Dee Belemnite (VPDB) standard. All calculations and statistical analyses were performed in R version 4.3.0 (R Core Team, 2023). For each batch culture, the nitrate-to-silicate uptake ratio was determined from the slope of a linear regression between nitrate and silicate concentrations, using only data points collected for before the addition of supplemental silicate to the culture.

Assuming that ^{15}N fractionation during nitrate assimilation in the closed-system batch cultures follows Rayleigh-type behavior/systematics (Mariotti *et al.*, 1981), the N-isotope fractionation, $\varepsilon_{biomass/NO3}$, was estimated as the slope of the linear relationship between the natural logarithm of the N isotopic ratio of nitrate ($^{15}N/^{14}N$) and the fraction of nitrate remaining in the medium (*f*). This relationship was modelled using the *lm* function in R. The intercept of this

regression approximates the initial nitrate $\delta^{15}N$ value, i.e., when $f = 1$ ($\delta^{15}N_{f1}$). Using $\varepsilon_{biomass/NO3}$ and $\delta^{15}N_{f1}$ we calculated the expected $\delta^{15}N$ value of biomass (i.e., the accumulated product) as a function of f, using the Rayleigh-based equation:

$$\delta^{15} N_{pred.biomass} = \delta^{15} N_{f1} - \varepsilon_{biomass\,/\,NO3} \times \frac{f \ln f}{1-f}$$

To evaluate whether the integration of nitrate $\delta^{15}N$ values into biomass occured predictably according to Rayleigh dynamics, we tested whether the slope of the relationship between predicted and measured biomass $\delta^{15}N$ values differed significantly from 0 and 1. Additionally, to assess how faithfully biomass $\delta^{15}N$ values are recorded in frustule-bound N, we also tested if the slope of the regression between $\delta^{15}N$ values of frustule-bound N and those of bulk biomass differed significantly from 0 and 1. These (linear) regressions were also conducted using the *lm* function in R. The N-isotopic offset between $\delta^{15}N$ values of frustule-bound N and biomass was calculated as $\varepsilon_{DB/biomass} = \alpha - 1$, and $\alpha = (\delta^{15}N_{DB} + 1)/(\delta^{15}N_{biomass} + 1)$, expressed in ‰ (Coplen, 2011). We then related $\varepsilon_{DB/biomass}$ values to the nitrate drawdown (f) to determine whether $\varepsilon_{DB/biomass}$ changed with batch culture progression. The slopes of these relationships were then compared to $\varepsilon_{biomass/NO3}$, but this analysis was limited to batch cultures with at least four $\varepsilon_{DB/biomass}$ values (Table 1).

All the above analyses excluded samples from the ^{15}N-labeled nitrate addition experiments. For these experiments, the biomass $\delta^{15}N$ values after label addition were estimated by isotope mass balance, considering f values and the $\delta^{15}N$ values of both the newly synthesized biomass (after addition of the ^{15}N-labeled nitrate), and the pre-existing accumulated biomass (before ^{15}N-label addition).

Results

Nutrient concentrations during batch cultures

Table 1: Overview of initial and final nitrate concentrations, Si:NO_3^- uptake ratio, frustule N content, C and N content, and batch culture duration. Values are reported as mean ± SD where applicable. bSi, biogenic silica

Species	No.	Starting [NO_3^-] (uM)	Final [NO_3^-] (uM)	Si:NO_3^- uptake ratio	Frustule N content (nmol N mg $^{-1}$ bSi)	Biomass C fraction (g g $^{-1}$)	Biomass N fraction (g g^{-1})	Number of frustule samples	Culture duration (d)	Notes
Aulacoseira granulata	1	195	56	2.6	14.2 ± 1.6	0.19 ± 0.02	0.031 ± 0.001	3	13	
	2	196	14	2.1	12.4 ± 0.5	0.22 ± 0.04	0.035 ± 0.002	3	13	
	3	191	0	2.6	12.8 ± 0.7	0.20 ± 0.02	0.037 ± 0.006	4	14	With TES buffer
	4	196	0	1.8	15.7 ± 5.9	0.18 ± 0.02	0.035 ± 0.004	5	15	With TES buffer
	5	203	0	2.3	9.0 ± 0.5	0.16 ± 0.01	0.031 ± 0.003	6	15	^{15}N-labeled nitrate addition
	6	208	1	1.9	9.9 ± 0.7	0.18 ± 0.02	0.033 ± 0.002	6	12	^{15}N-labeled nitrate addition
Fragilaria capucina	1	194	45	2.2	13.2 ± 1.0	0.23 ± 0.01	0.030 ± 0.002	3	22	
	2	194	21	2.3	14.3 ± 2.6	0.26 ± 0.03	0.032 ± 0.001	3	21	
	3	185	1	2.9	9.3 ± 1.3	0.20 ± 0.03	0.028 ± 0.002	5	15	With TES buffer
	4	194	6	2.6	8.8 ± 1.2	0.19 ± 0.03	0.028 ± 0.002	6	17	With TES buffer
	5	205	2	1.5	7.1 ± 2.3	0.21 ± 0.03	0.030 ± 0.005	6	21	^{15}N-labeled nitrate addition
	6	200	0	1.9	6.0 ± 1.3	0.22 ± 0.02	0.028 ± 0.003	6	21	^{15}N-labeled nitrate addition
Chaetoceros calcitrans	1	512	4	0.5	17.6 ± 1.5	0.15 ± 0.03	0.028 ± 0.005	4	8	
	2	502	4	0.4	15.6 ± N/A	0.14 ± 0.06	0.025 ± 0.011	4	8	
	3	500	2	0.7	4.1 ± 0.7	0.13 ± 0.04	0.027 ± 0.007	4	7	
Coscinodiscus radiatus	1	509	27	4.1	2.2 ± 0.4	0.11 ± 0.01	0.016 ± 0.002	5	47	
	2	513	2	4.4	1.7 ± 0.3	0.12 ± 0.02	0.016 ± 0.002	5	47	

Batch cultures lasted 12-15 days for *A. granulata*, 15-22 days for *F. capucina*, 7-8 days for *C. calcitrans*, and 47 days for *C. radiatus* (Table 1; Fig. S1 and S2). In 14 out of 17 batch culture experiments, nitrate was consumed to less than 0.1 *f*. Silicate to nitrate uptake ratios were highly variable among species; for *C. radiatus* the Si:NO_3^- uptake ratio was between 4.1 and 4.4, while

these were between 1.5 and 2.9 for the freshwater species, and between 0.4 and 0.7 for *C. calcitrans* (Table 1).

Fractionation of nitrate N isotopes during nitrate assimilation

The ^{15}N fractionation of nitrate upon assimilation ($\varepsilon_{biomass/NO3}$), varied substantially among species (Fig. 1). Largest $\varepsilon_{biomass/NO3}$ values were found for *C. radiatus* (-13.8 ±0.2 ‰), followed by *A. granulata* (-10.8 ±1.0 ‰), and *C. calcitrans* (-3.1 ±0.5 ‰), with the smallest values found for *F. capucina* (-1.9 ±0.2 ‰).

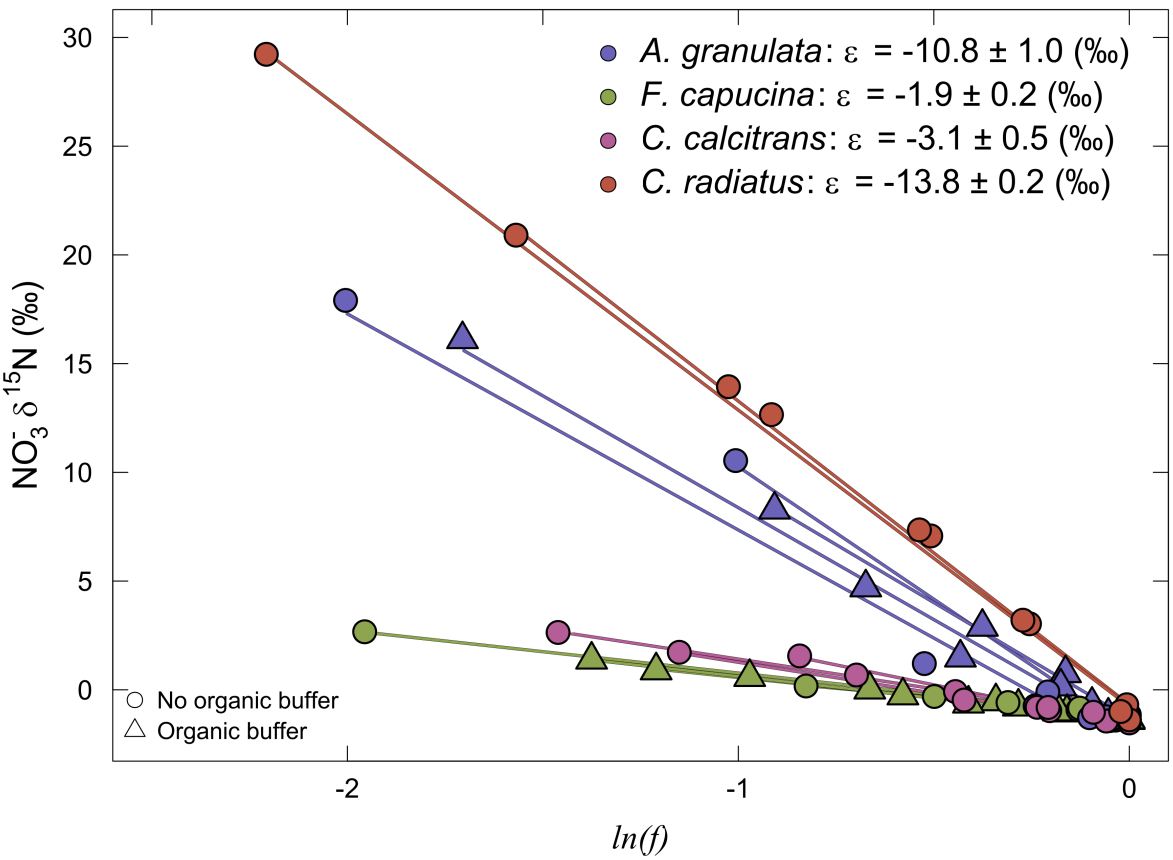

Figure 1: Nitrate ^{15}N fractionation ($\varepsilon_{biomass/NO3}$) upon assimilation by different diatom species. ε values given in the legend represent species mean ± SD based on slopes of the linear regressions. Note that ε values were calculated using nitrogen isotope ratios, not $\delta^{15}N$ values, but for ease of interpretation, the regressions were visualized on the $\delta^{15}N$ scale instead. ε values reported for each species are displayed ± 1sd, where the sd is based on ε values from culture replicates.

Biomass $\delta^{15}N$ and $\delta^{13}C$ values

Predicted biomass $\delta^{15}N$ values were very similar to measured biomass $\delta^{15}N$ values (Fig. 2) with a slope of 0.95 ($p < 0.001$ for slope =/= 0), close to, but significantly different from 1 ($p = 0.026$ for slope =/= 1). Importantly, the explanatory power of this relationship was very high ($R^2 = 0.97$), so that predicted biomass $\delta^{15}N$ values could explain nearly all of the observed variation in measured biomass $\delta^{15}N$ values.

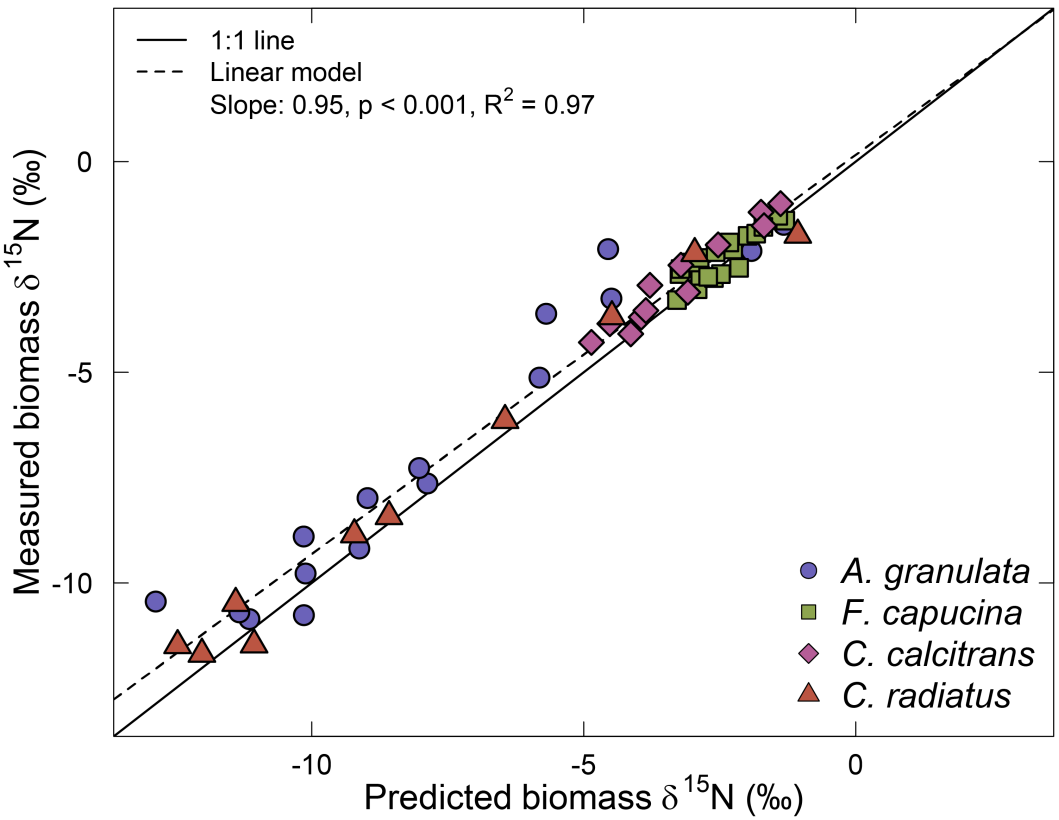

Figure 2: Comparison of predicted versus measured biomass $\delta^{15}N$ values. Predicted biomass $\delta^{15}N$ values are calculated as the integrated product based on the ^{15}N fractionation upon nitrate assimilation and the fraction of nitrate remaining when the sample was taken.

As a result of $\varepsilon_{biomass/NO3}$, at high *f* values, biomass $\delta^{15}N$ values were lowest in *A. granulata* and *C. radiatus* around -11 to -12 ‰, while those of *F. capucina* and *C. calcitrans* were never lower than -5 ‰ (Fig. 3). Upon (near) complete consumption of nitrate in the medium, all species approached biomass $\delta^{15}N$ values close to starting nitrate $\delta^{15}N$ values of around -1.4 ‰ (Fig. 3).

For *A. granulata*, *F. capucina* and *C. calcitrans*, biomass $\delta^{13}C$ values increased with decreasing *f* (Fig. S3), with the magnitude of the increase being larger for species which more rapidly consumed the nitrate in the medium (Table 1). For *C. radiatus*, there was no strong increase in biomass $\delta^{13}C$ values during the batch culture, but the values were elevated compared to the lowest biomass $\delta^{13}C$ values in the other species.

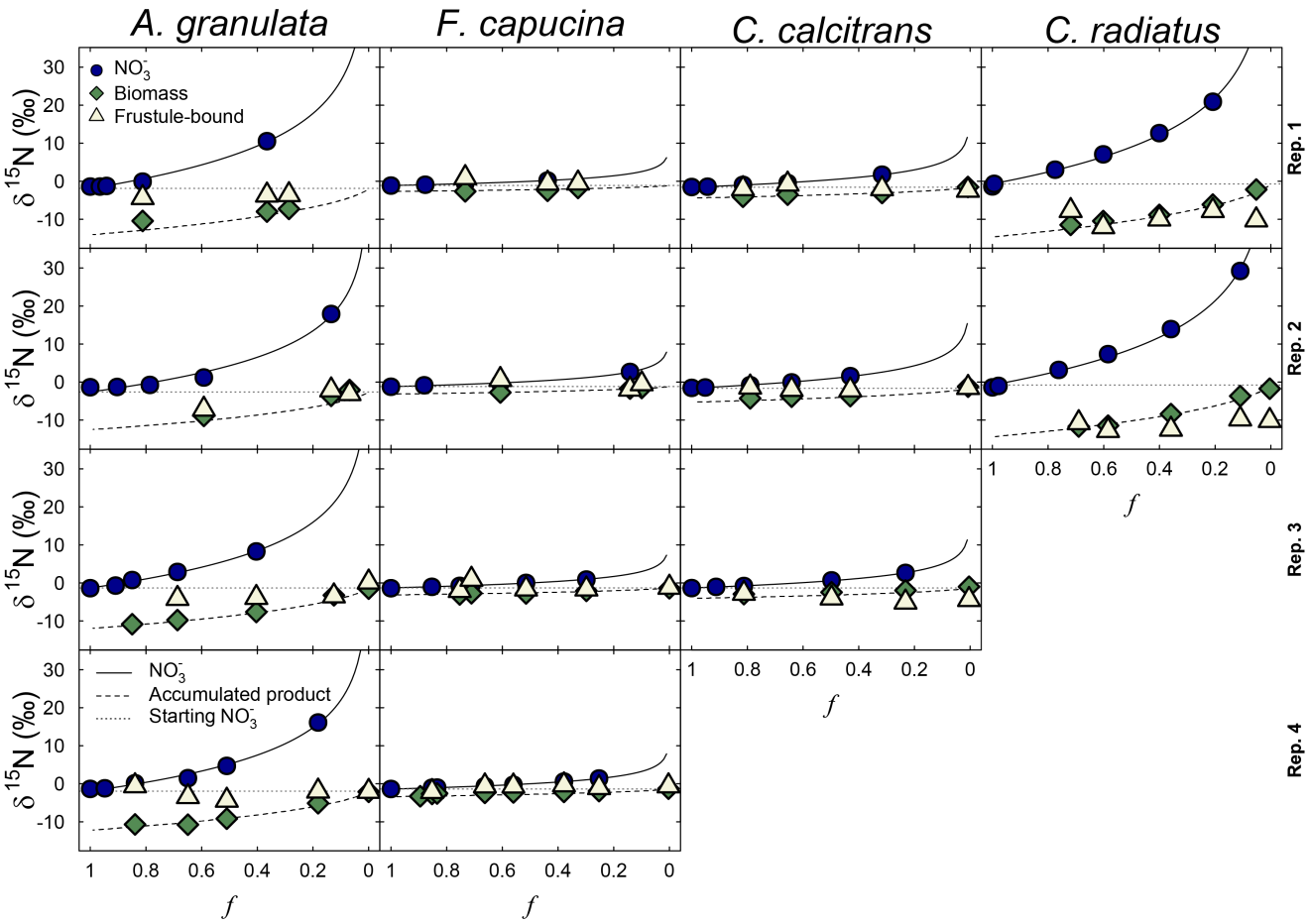

Figure 3: $\delta^{15}N$ values of nitrate (blue circles), biomass (green diamonds) and frustule-bound N (white triangles plotted against the fraction of nitrate remaining in the medium (f). Panels represent results from single batch cultures, which are organized by species (columns) and culture replicates (rows). Solid, dashed, and dotted lines represent theoretical lines for $\delta^{15}N$ values of nitrate, accumulated biomass, and starting nitrate, respectively. For A. granulata *and* F. capucina*, culture replicates 3 and 4 were grown in medium containing TES buffer.*

Diatom frustule-bound $\delta^{15}N$ values

Typically, while biomass $\delta^{15}N$ values increased with decreasing *f*, $\delta^{15}N_{DB}$ values did not (Fig. 3). Linear regression of $\delta^{15}N_{DB}$ values against biomass $\delta^{15}N$ values across all species shows a significant relationship ($p = 0.003$ for slope =/= 0; Fig. 4). However, the slope of this relationship was significantly different from 1 ($p < 0.001$ for slope =/= 1) and the explanatory power of the relationship was relatively low ($R^2 = 0.32$). Additionally, the significance and explanatory power of this relationship will be diminished when data is analyzed on a species- or culture-specific level.

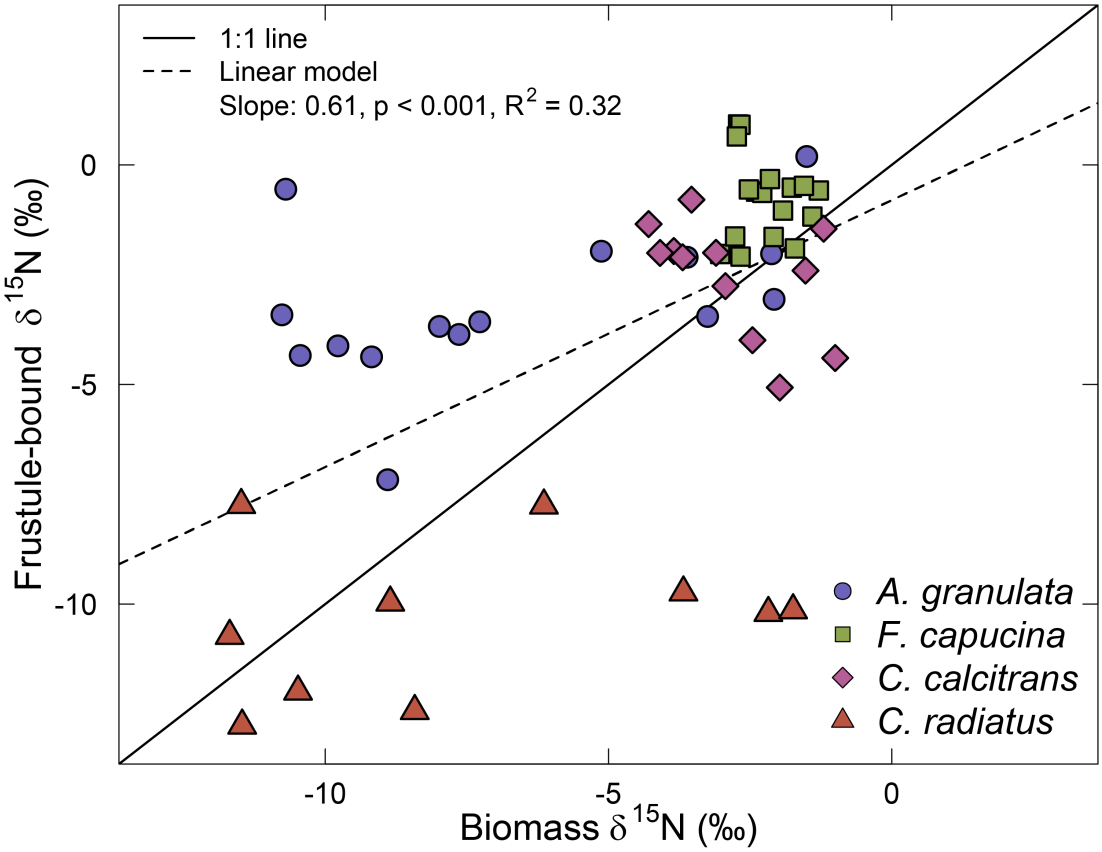

Figure 4: Comparison between frustule-bound and biomass $\delta^{15}N$ values. Linear regression (dashed line) was determined across all species and batch cultures.

The isotopic offset between $\delta^{15}N_{DB}$ values and biomass $\delta^{15}N$ values, as $\varepsilon_{DB/biomass}$, was highly variable, from +10.3 to -8.4 ‰ depending on the species (Fig. 5). Moreover, in most batch cultures, $\varepsilon_{DB/biomass}$ decreased with decreasing *f*. The magnitude of this decrease was dependent on

the species, with the strongest decreases for *A. granulata* and *C. radiatus*, and weaker decreases for *F. capucina* and *C. calcitrans*. In *A. granulata*, $\varepsilon_{DB/biomass}$ decreased from between +10 and +6 ‰ around 0.8 *f* to around 0 ‰ when *f* reached zero, while this was from +5 ‰ to -8 ‰ between *f* 0.7 and 0 for *C. radiatus*. In *F. capucina* and *C. calcitrans*, $\varepsilon_{DB/biomass}$ decreased by roughly 4 ‰ with *f* decreasing from 0.8 to 0. We further quantified the change in $\varepsilon_{DB/biomass}$ along the *f* gradient as a linear regression, where the slope represents the change in $\varepsilon_{DB/biomass}$ along *f*. This showed that this change was inversely proportional to $\varepsilon_{biomass/NO3}$ (Fig. S4).

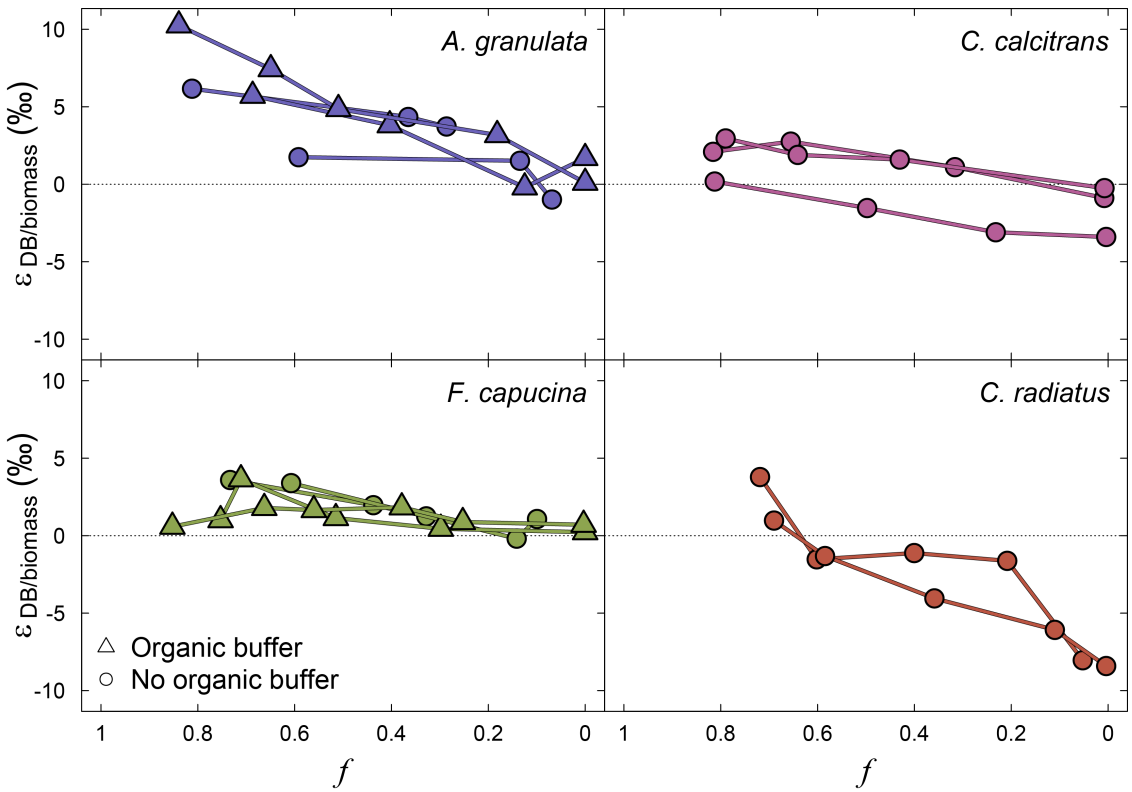

Figure 5: Isotopic offset between biomass and frustule-bound N (calculated as $\varepsilon_{DB/biomass}$) progressing along the batch culture (as fraction of nitrate remaining; f). Points represent single measurements and lines connect sequential measurements from a single batch culture.

C and N content (Table 1), and the ratio between them, could not explain variation in $\varepsilon_{DB/biomass}$ within most species, except for *A. granulata*, where lower C contents and C/N ratios were associated with lower $\varepsilon_{DB/biomass}$ values ($p = 0.045$ and $p = 0.049$, respectively).

Changes in biomass and frustule-bound $\delta^{15}N$ values in response to high-$\delta^{15}N$ nitrate additions

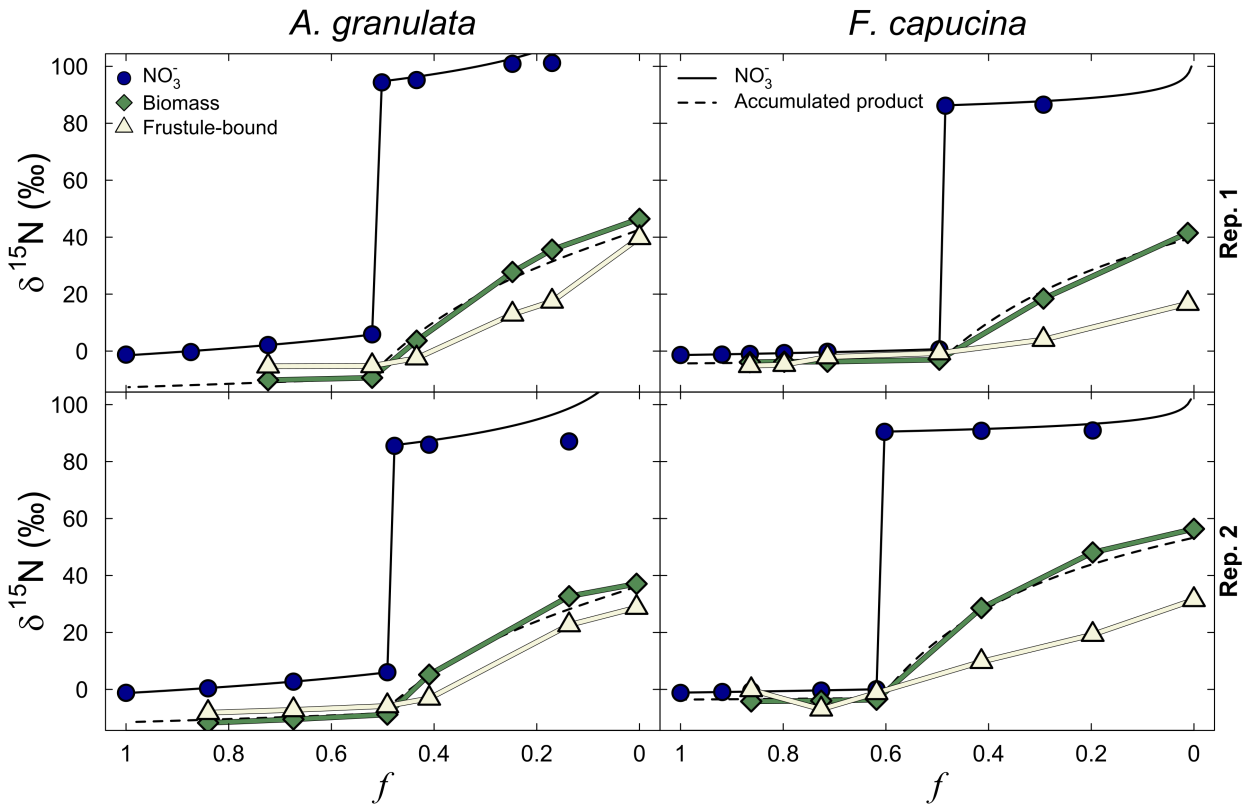

Figure 6: $\delta^{15}N$ values of nitrate, biomass and frustule-bound N in response to the spiked nitrate $\delta^{15}N$ when roughly half of total nitrate was consumed. Dashed lines represent an estimation of biomass $\delta^{15}N$ values (as accumulated product), which was approached as a mass balance equation after the nitrate $\delta^{15}N$ spike.

In an experiment to assess the integration of N isotopes from nitrate into biomass and frustule-bound N, we manipulated medium nitrate $\delta^{15}N$ values, when roughly half of the initial nitrate pool was consumed, increasing nitrate concentrations by just 1-2 μM. Spiked nitrate $\delta^{15}N$ values upon ^{15}N-labeled nitrate addition were between 85.5 ‰ and 94.4 ‰ (Fig. 6). Both biomass and diatom frustule-bound $\delta^{15}N$ values clearly responded to the addition of ^{15}N-labeled nitrate during batch cultures. The $\delta^{15}N$ values of biomass increased relatively close to predictions of $\delta^{15}N$ of an accumulated product. Frustule-bound $\delta^{15}N$ values also increased but were always distinctly lower than those of biomass. Additionally, $\varepsilon_{DB/biomass}$ values were species-specific, with *A. granulata* showing smaller offsets compared to *F. capucina*. Upon complete nitrate consumption

$\varepsilon_{DB/biomass}$ values were between -6.4 and -8.0 ‰ for *A. granulata*, and between -23.6 and -23.8 ‰ for *F. capucina*. Based on the $\delta^{15}N$ values of the samples prior to, and the first samples taken after addition of ^{15}N-labeled nitrate, the slopes of the relationship between biomass and frustule-bound $\delta^{15}N$ values were relatively shallow in both species, indicating that biomass $\delta^{15}N$ values initially increased more than those of frustule-bound $\delta^{15}N$ values (Fig. 7). After these initial samples, for *A. granulata*, the slope of this relationship approached 1 (0.93, $p = 0.55$ for slope =/= 1), whereas for *F. capucina* the slope remained smaller than 1 (0.66, $p = 0.04$ for slope =/= 1). For *A. granulata*, the initial samples were taken at roughly 3.6 and 5.5h after ^{15}N-labeled nitrate was added, resulting in a fractional consumption of 0.07*f* nitrate (Fig. S2). By contrast, for *F. capucina*, this was 21.6 and 22.8h after spiking, resulting in a fractional consumption of 0.19*f* nitrate. Throughout the experiment, empty frustule counts relative to frustules that contained biomass were consistently low (< 3 %; Table S1).

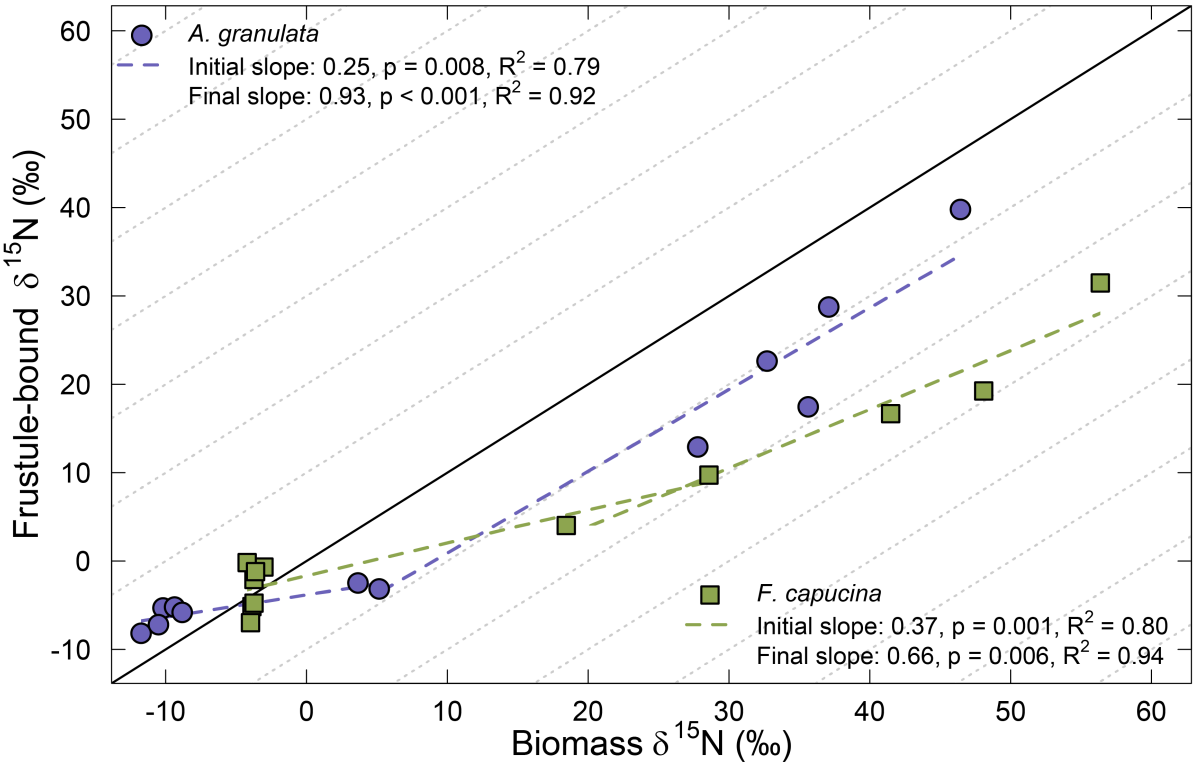

Figure 7: Frustule-bound $\delta^{15}N$ values plotted against biomass $\delta^{15}N$ values of samples taken in the experiment with ^{15}N-labeled nitrate. Slopes (dashed lines) were determined on a species-specific basis separated by color. Initial slopes were calculated between samples before addition of ^{15}N-labeled nitrate and the first two samples collected after addition of ^{15}N-labeled nitrate. The 'final slopes' were calculated based on data from samples after addition of ^{15}N-labeled nitrate. The solid line represents a slope of 1 with intercept 0. Dotted lines represent a slope of 1 with intercepts sequentially offset by 10 ‰.

Discussion

Meaningful interpretation of $\delta^{15}N$ values of diatom frustule-bound organic N ($\delta^{15}N_{DB}$) stored in sedimentary records relies on proper understanding of the integration of N stable isotopes from the source N pool into diatom biomass, and subsequently into frustule-bound organic N. Here we present new data from mono-specific diatom cultures that illustrates the relationship of $\delta^{15}N$ values among nitrate, biomass and frustule-bound organic N in two freshwater and two marine diatom species. The results presented from these cultures show that $\delta^{15}N_{DB}$ values can be substantially different from diatom biomass $\delta^{15}N$ values, and this further depends on species and on batch culture progression. Moreover, we performed experiments where nitrate $\delta^{15}N$ values in the medium were manipulated during batch culture experiments, which showed that integration of nitrate $\delta^{15}N$ values was more rapid in biomass compared to frustule-bound organic N, and the extent of this difference was species-dependent. However, these results could not explain the observed discrepancies between biomass and frustule-bound $\delta^{15}N$ values in the experiments at natural abundance $\delta^{15}N$ levels, suggesting that this is primarily driven by internal biochemical ^{15}N fractionation.

Incorporation of nitrate $\delta^{15}N$ signatures into biomass and frustule-bound N

Overall, we find that the ^{15}N fractionation upon assimilation of nitrate ($\varepsilon_{biomass/NO3}$) can vary substantially among species, but it is relatively stable within species in the conditions tested (Fig. 1), as has also been shown in other studies (Needoba *et al.*, 2003). Moreover, we observed good agreement between measured biomass $\delta^{15}N$ values and predicted biomass $\delta^{15}N$ values (as accumulated product) based on $\varepsilon_{biomass/NO3}$ (Fig. 2 & 3). Therefore, ^{15}N fractionation of nitrate and subsequent integration into biomass followed predictable Rayleigh type fractionation in our batch culture experiments.

Previous studies using samples from the natural environment showed that although there was correlation between biomass and frustule-bound $\delta^{15}N$ values, neither of these were correlated to those of the surrounding nitrate, which was likely due to uptake of substantial amounts of ammonium with distinct $\delta^{15}N$ values (Morales *et al.*, 2014; Robinson *et al.*, 2020). In controlled batch cultures with nitrate as the only inorganic N source, $\delta^{15}N_{DB}$ values are expected to follow the increasing $\delta^{15}N$ values of accumulating biomass driven by $\varepsilon_{biomass/NO3}$. Indeed, in our controlled batch culture studies, we find a significant relationship between $\delta^{15}N$ values of frustule-bound N and biomass across the different species and culture replicates (Fig. 4). However, it is important to note that the slope of this relationship is significantly different from 1, and making the same comparison within species or culture replicates, the relationship disappears. Moreover, the unexpectedly low explanatory power of this relationship ($R^2 = 0.32$) suggests that only around one third of the observed variation in $\delta^{15}N_{DB}$ values can be explained by those of biomass. Thus, the increase in biomass $\delta^{15}N$ values induced by increasing fractional nitrate consumption was not strictly followed by a corresponding change in $\delta^{15}N_{DB}$ values. This implies that $\delta^{15}N_{DB}$ does not directly represent the $\delta^{15}N$ values of an accumulated product in batch cultures, and the interpretation of $\delta^{15}N_{DB}$ may not be a pristine reflection of biomass $\delta^{15}N$ values.

The offset between frustule-bound and biomass $\delta^{15}N$ values changes with batch culture progression

In the batch culture experiments, the isotopic offset between frustule-bound and biomass $\delta^{15}N$ values ($\varepsilon_{DB/biomass}$) was not constant and decreased with batch culture progression (Fig. 5). This is mostly the result of the species-specific increase in biomass $\delta^{15}N$ values with fractional nitrate consumption, while $\delta^{15}N_{DB}$ values remained more stable (Fig. 3). Such relatively stable $\delta^{15}N_{DB}$ values could imply that the organic N found in frustules originates from a source of N that

is unaltered throughout the batch culture. It has been proposed that synthesis of frustule-bound organic N molecules can occur well before frustule synthesis as a potential explanation for low $\delta^{15}N_{DB}$ values of *Cheatoceros* resting spores relative to frustules from vegetative cells (Dove *et al.*, 2025). From batch culture experiments with natural abundance nitrate $\delta^{15}N$ values, it is difficult to assess if organic N in newly formed frustules undergoes variable biochemical ^{15}N fractionation and/or isotopically represents early culture stages, which is further discussed in a later section. Irrespective of this, the change in $\varepsilon_{DB/biomass}$ values may provide interesting perspectives on results from batch culture experiments in previous studies.

The results from Horn *et al.*, (2011) suggest a positive relationship between $\varepsilon_{DB/biomass}$ and $\varepsilon_{biomass/NO3}$. By comparison, our results also show that $\delta^{15}N_{DB}$ values can be strongly offset from biomass $\delta^{15}N$ values in species with large $\varepsilon_{biomass/NO3}$ values and are generally small in species with small $\varepsilon_{biomass/NO3}$ values (Fig. 1 & 5). However, it is important to consider that $\varepsilon_{DB/biomass}$ was not constant in our cultures (Fig. 3 & 5), and it appears that the magnitude of change in $\varepsilon_{DB/biomass}$ during batch culture progression is also proportional to $\varepsilon_{biomass/NO3}$ (Fig. S4). As such, the drivers that cause the variable $\varepsilon_{DB/biomass}$ values could be related to physiological processes involved in nitrogen assimilation and/or metabolism.

The species used in our study represent a large range in levels of silicification, with *C. radiatus* having Si:NO_3^- uptake ratios larger than 4, while between 0.4 and 0.7 for *C. calcitrans*, and between 1.5 and 2.9 for the freshwater species (Table 1). In line with previous suggestions (Robinson *et al.*, 2025), the heavily silicified *C. radiatus* was the only species with $\delta^{15}N_{DB}$ values more consistently below biomass $\delta^{15}N$ values (Fig. 4 & 5). However, even though *A. granulata* and *F. capucina* had similar Si:NO_3^- uptake ratios (Table 1), the observed $\varepsilon_{DB/biomass}$ values are substantially different between the two species (Fig. 5). Moreover, we find that $\varepsilon_{DB/biomass}$ values

were highly variable within a single batch culture, changing from up to +10 ‰ down to around 0 ‰ in the case of *A. granulata*, or from up to nearly +5 ‰ down to -8 ‰ in *C. radiatus*. Depending on the species, the silicification rates may change throughout the batch culture as Si concentrations decrease (Kudo, 2003). However, we still find substantial changes in $\varepsilon_{DB/biomass}$ values even when changes in Si concentration are relatively small (Fig. 5; Fig. S1 & S2). Thus, the results from our batch cultures do not fit the relationship between Si:NO_3^- uptake rates and $\varepsilon_{DB/biomass}$ as suggested by Robinson *et al*. (2025).

In previous work, it was difficult to gauge whether $\varepsilon_{DB/biomass}$ values were stable or varied during batch cultures, since cultures were terminated before complete consumption of nitrate (Horn *et al.*, 2011), or only a single sample was collected for $\delta^{15}N_{DB}$ analyses (Jones *et al.*, 2022; Robinson *et al.*, 2025). As such, the interpretation of the previously obtained results from culturing studies may be obscured if $\varepsilon_{DB/biomass}$ values cannot be assumed constant throughout the batch culture. Importantly, for the interpretation of $\delta^{15}N_{DB}$ values from diatom culture studies, our results imply that $\delta^{15}N_{DB}$ values do not clearly follow the dynamics of an accumulating product in a Rayleigh-type system. The resulting changes in $\varepsilon_{DB/biomass}$ values with batch culture progression are likely driven by (1) changes in ^{15}N fractionation associated with changing biochemical reactions during N metabolism, and/or (2) differences in the timing of N isotope integration between $\delta^{15}N_{DB}$ and biomass $\delta^{15}N$ values through utilization of N-reservoirs established early on in the batch culture. We further explored the importance of the latter process in separate batch culture experiments where ^{15}N-labeled nitrate was added when roughly half of the initial nitrate concentration was remaining.

Slower nitrate isotope incorporation into the frustule-bound N pool does not explain $\varepsilon_{DB/biomass}$ variation

The observed relatively constant $\delta^{15}N_{DB}$ values along the batch culture progression (Fig. 3) could suggest that $\varepsilon_{DB/biomass}$ is mostly driven by utilization of an isotopically stable N reservoir for frustule-bound organic N synthesis. To test this hypothesis, an experiment with high nitrate $\delta^{15}N$ values showed that while biomass $\delta^{15}N$ values increased along the predicted path, $\delta^{15}N_{DB}$ values also increased but were consistently lower than those of biomass (Fig. 6; Fig. 7). This could be caused by high, or changing, numbers of empty frustules relative to biomass-filled frustules. However, the relative abundance of empty frustules was consistently low (Table S1).

After addition of ^{15}N-labeled nitrate, the clearly lower $\delta^{15}N$ values of frustule-bound N compared to biomass indicate that, not all, but a (small) part of the organic N in frustules originates from before the manipulation of nitrate $\delta^{15}N$ values. Moreover, it appears that the magnitude of this effect is likely species-specific, as frustule-bound $\delta^{15}N$ values relative to biomass were substantially lower in *F. capucina* (-23.6 ‰) compared to *A. granulata* (-7.2 ‰) upon complete nitrate consumption. More specifically, after 3.6 and 5.5h (with fractional nitrate consumption of 0.07*f*) following addition of ^{15}N-labeled nitrate, frustule-bound $\delta^{15}N$ values in *A. granulata* followed those of biomass with a slope not significantly different from 1 (Fig. 7; Fig. S2; $p < 0.001$ for slope =/= 0 and $p = 0.55$ for slope =/= 1). By contrast, for *F. capucina*, this took much longer, and the slope between biomass and frustule-bound $\delta^{15}N$ values did not yet approach 1 in the given experiment time ($p = 0.006$ for slope =/= 0; $p = 0.04$ for slope =/= 1). Therefore, logically, assimilation of ^{15}N-labeled nitrate instantaneously impacts biomass $\delta^{15}N$ values, while the pool of organic N that is used for frustule-bound N synthesis requires a certain amount of time to be replaced with new, ^{15}N-labeled organic N. Alternatively, it is possible that in the period where we

observed little change in $\delta^{15}N_{DB}$ values, but a large change in biomass $\delta^{15}N$ values, no new frustules were synthesized. However, at least in *F. capucina* some new frustules must have been formed during this time based on the Si consumption (Fig. S2). As such, our results imply that frustule-bound organic N originates from a reservoir that integrates (slightly) slower, leading to asynchronous integration of nitrate $\delta^{15}N$ values into frustule-bound N compared to overall biomass.

Diatom-internal N reservoirs relevant to $\delta^{15}N_{DB}$ values could take several forms: intracellular nitrate (Stief *et al.*, 2022), monomers (amino acids) (Admiraal *et al.*, 1986), N/C-storage compounds such as urea and creatin-P (Allen *et al.*, 2006; Parker *et al.*, 2008), or as the silicate precipitating organic compounds prior to incorporation into the frustule (Kotzsch *et al.*, 2017; Tesson *et al.*, 2017). Stored nitrate originating from early in the culture progression is unlikely to influence $\delta^{15}N_{DB}$ values independently of biomass, since assimilation of nitrate into organic compounds is not expected to occur via a temporally or spatially distinct pathway dedicated to frustule-bound organic N synthesis.

Once assimilated into amino acids, the building blocks of proteins and polyamines, including those integrated into diatom frustules, N can be stored in different organic N forms. In higher plants, amino acid turnover times can be less than 1 hour (Racusen & Foote, 1960), and in diatoms, substantial ^{15}N enrichment in amino acids has been observed 1 hour after ^{15}N-label addition (Smith *et al.*, 2019). These rapid N turnover rates imply that amino acids are unlikely to retain isotopically distinct signatures over extended periods. Therefore, it is improbable that amino acid reservoirs serve as the source of delayed or asynchronous integration of ^{15}N-labeled nitrate into frustule-bound organic N compared to biomass.

Many products of the diatom urea cycle can act as N-reservoirs, such as urea and creatine-P (Allen *et al.*, 2006; Parker *et al.*, 2008). The consequences for frustule-bound $\delta^{15}N$ values of these N-reservoirs depend on the extent of N-reservoir buildup and its utilization, which likely vary among species identity and growth conditions. Under the assumption that utilization of such organic N-reservoirs would occur mainly during N-limitation, it is unlikely that these were specifically utilized as a source of ^{15}N-depleted N for frustule-bound organic N synthesis, as N-limitation only occurred towards the very end of the batch culture.

Pools of certain frustule-bound organic compounds could be established prior to frustule-synthesis (Kotzsch *et al.*, 2017; Tesson *et al.*, 2017). Moreover, this was suggested as a potential explanation for low $\delta^{15}N$ values of frustule-bound N in *Chaetoceros* resting spores relative to frustules from vegetative cells (Dove *et al.*, 2025). The presence of substantial amounts of frustule-bound organic compounds prior to frustule synthesis would require additional time to be replaced with new ^{15}N-labeled organic compounds, affecting the integration of nitrate $\delta^{15}N$ values into frustule-bound N.

Overall, the results from the ^{15}N-labeled nitrate addition experiments (Fig. 6 & 7) imply that the organic N in frustules is synthesized from an organic N pool that requires a specific amount of time to be replaced by newly assimilated N. This time-window was provenly species-dependent, as slower growing species required longer periods of time to replace the N reservoirs with newly assimilated N (Table 1, Fig. 7). Therefore, integration of nitrate $\delta^{15}N$ values into frustule-bound $\delta^{15}N$ values will take a species-specific amount of time longer than the integration into biomass $\delta^{15}N$ values. This should be carefully considered in future batch culture experiments, since it cannot be assumed that $\delta^{15}N_{DB}$ values integrate over the exact same time window as biomass $\delta^{15}N$ values. Moreover, this result further complicates the interpretation of previous batch culture

studies, where $\delta^{15}N_{DB}$ values were determined at a single timepoint (Jones *et al.*, 2022; Robinson *et al.*, 2025).

With the slightly slower integration of nitrate $\delta^{15}N$ values into frustule-bound N compared to biomass, $\delta^{15}N$ values would still be expected to reflect the increase in biomass $\delta^{15}N$ values in batch cultures at natural abundance $\delta^{15}N$ values, but with an offset in time or *f*. Yet, in our batch cultures, $\delta^{15}N_{DB}$ values showed hardly any increase at all (Fig. 3). As such, to explain the observed changes in $\varepsilon_{DB/biomass}$ values (Fig. 5), internal ^{15}N fractionation likely varied with batch culture progression, which will be discussed next.

Biochemical ^{15}N fractionation could substantially affect frustule-bound $\delta^{15}N$ values

Changes in growth conditions are an inherent feature of batch cultures, since nutrient concentrations decrease, while demands for nutrients (including inorganic C) increase with increasing cell density. The increased cell density additionally results in shading of the inner medium volume leading to decreased light intensity. We found that biomass $\delta^{13}C$ values progressively increased (or were constantly elevated in the case of *C. radiatus*) (Fig. S3), which implies (1) a higher degree of inorganic C consumption (Degens *et al.*, 1968; Deuser, 1970; Fry, 1996; Burkhardt *et al.*, 1999), (2) an induction of a C concentration mechanism (Sharkey & Berry, 1985), and/or (3) enhanced C fixation through phosphoenolpyruvate carboxylase as response to increased assimilation of ammonium (Guy *et al.*, 1989). Therefore, the observed biomass $\delta^{13}C$ values are a general example of the progressive changes in growth conditions that inherently occur during batch cultures. Overall, the initially higher, and subsequently decreasing, frustule-bound $\delta^{15}N$ values relative to biomass (Fig. 5) could be a result of growth condition driven changes in (1) the frustule-bound organic compound matrix, and/or (2) ^{15}N-fractionating reactions during frustule-bound organic compound synthesis, and/or (3) ^{15}N-fractionating reactions in the amino

acid synthesis pathways. In the following we address potential mechanisms by which $\varepsilon_{DB/biomass}$ may or may not have changed.

Regarding (1): if the frustule-bound organic compound matrix changed during the batch cultures, associated with a shift in contribution of N from precursor molecules with high $\delta^{15}N$ values to N with low $\delta^{15}N$ values, this would be reflected in $\delta^{15}N_{DB}$. It is currently not known if the frustule-bound organic compound matrix is plastic within species. Considering that the frustule-bound polyamine composition is highly species-specific (Bridoux & Ingalls, 2010; Bridoux *et al.*, 2012), the frustule-bound organic compound matrix is more likely to be driven by diatom phylogeny than by growth conditions.

Regarding (2): for proteins, it can be assumed that the ribosomal biosynthesis from amino acids does not isotopically discriminate (Werner & Schmidt, 2002). However, in higher plants, polyamine $\delta^{15}N$ values were determined to be very high relative to the amino precursor molecules, suggesting a high potential for ^{15}N fractionation during polyamine biosynthesis (Yoneyama *et al.*, 1998). Additionally, in diatom frustule-bound silaffins and polyamines, methylation of amine groups has been shown to occur (Sumper & Brunner, 2008; Kröger & Poulsen, 2008; Bridoux & Ingalls, 2010). Since such reactions involve the breaking of N-H and forming of N-C bonds, ^{15}N fractionation may be introduced here. This ^{15}N fractionation could be expressed if methylation of amine groups occurs around branching points within the synthesis pathway, and/or if the substrate-product reaction is incomplete. It has been shown that increased methylation enhances the ability to precipitate silicic acid (Robinson *et al.*, 2007), and this is known to vary among species (Bridoux *et al.*, 2012). However, whether or not a change in the degree of methylation of frustule-bound organic-N can occur within a species, resulting in variable ^{15}N fractionation as an explanation for the change in $\varepsilon_{DB/biomass,}$ remains unclear.

Regarding (3): to reveal potential ^{15}N fractionation processes prior to diatom frustule-bound organic compound synthesis, it is important to understand how and from which precursor molecules these are synthesized. Polyamines are synthesized from a putrescine or ornithine backbone, and polypropylene-imine (PPI) chains of species-dependent lengths, which are ultimately derived from methionine synthesized from aspartate (Bridoux & Ingalls, 2010; Lin *et al.*, 2024). As such, the dominant source of N in polyamines with chains consisting of more than two PPI units will be methionine. By comparison, the frustule-bound proteins such as silaffins and silacidins are rich in serine (Poulsen *et al.*, 2003; Richthammer *et al.*, 2011) which is produced during photorespiration, while others have been shown to be rich in glutamine and asparagine (Kotzsch *et al.*, 2017), which are more closely related to N assimilation. Under the assumption that metabolic fluxes can influence the extent of isotopic fractionation (Tcherkez, 2010), diatom metabolism likely plays an important role in shaping amino acid $\delta^{15}N$ values (Fig. 8) and therefore those of frustule-bound organic N compounds. Understanding the variation among amino acid $\delta^{15}N$ values and the processes that could influence these may provide a comprehensive overview of potential biochemical influences on frustule-bound $\delta^{15}N$ values.

Transamination and deamination reactions in the photorespiration cycle lead to relatively low $\delta^{15}N$ values of serine in photosynthetic organisms (Fig. 8) (Tcherkez & Hodges, 2008; Gauthier *et al.*, 2013; McCarthy *et al.*, 2013; McMahon & McCarthy, 2016; Takizawa *et al.*, 2017). Although photorespiration strongly impacts $\delta^{15}N$ values of amino acids that are relevant for frustule-bound protein synthesis (Fig. 8) (Tcherkez & Hodges, 2008; Tcherkez, 2010), variation in the photorespiratory flux in diatoms is likely kept to a minimum by C concentrating mechanisms (Clement *et al.*, 2016) and increased specificity of the RubisCO enzyme for CO_2 (Tortell, 2000; Kroth *et al.*, 2008). However, photorespiration in diatoms can be induced under high light

conditions (Parker *et al.*, 2004), meaning that there is potential for expression of a variable photorespiratory flux and could therefore affect diatom amino acid $\delta^{15}N$ values used for frustule-bound organic compound synthesis.

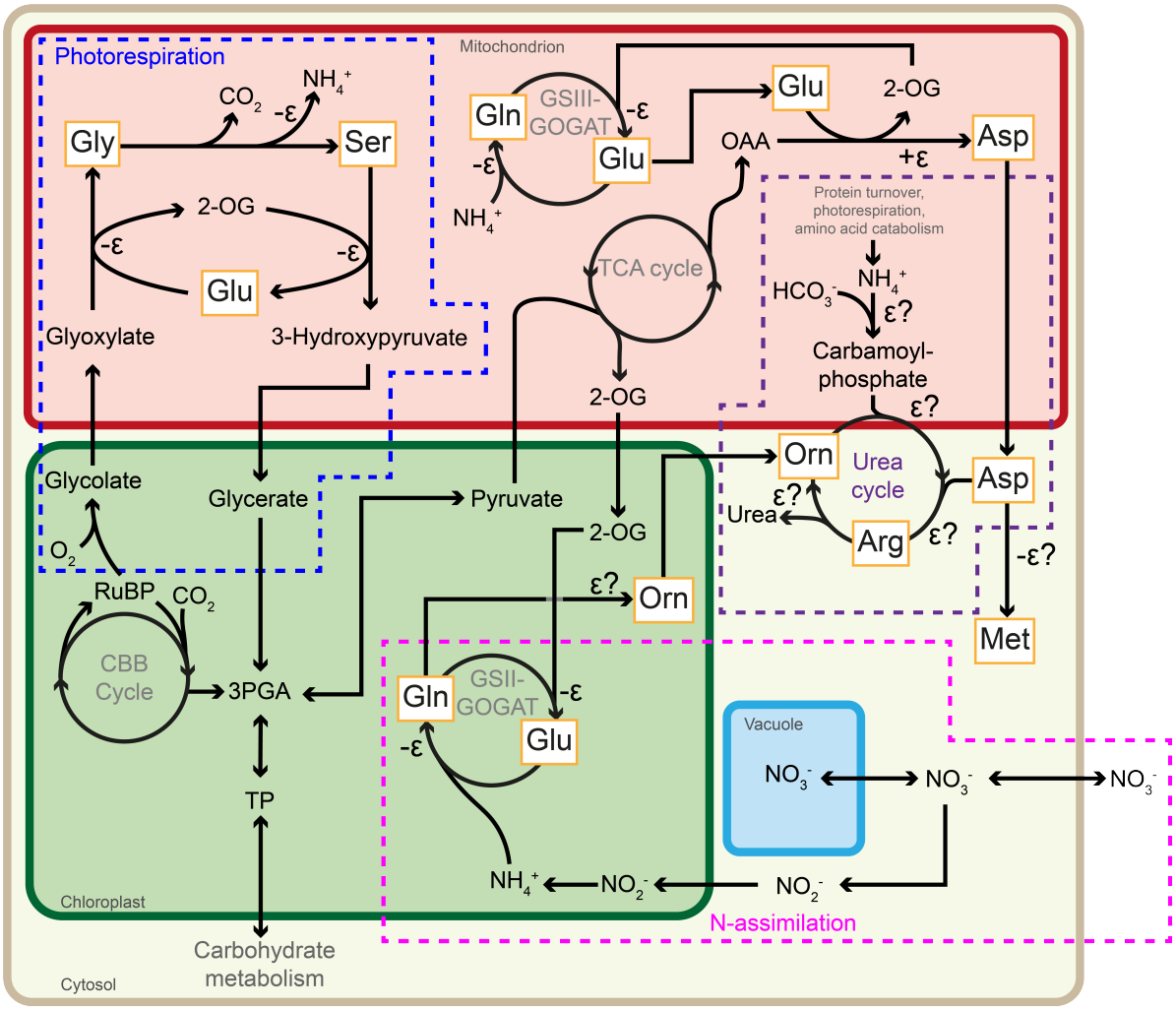

Figure 8: Schematic, simplified overview of the interaction between diatom C and N metabolism. Main areas of interaction are in N-assimilation (pink), photorespiration (blue) and the urea cycle (purple). Reactions involving N containing organic compounds are annotated with ε and a sign prefix, where -ε indicates a reaction resulting in lower product $\delta^{15}N$ values, and +ε indicates the opposite. In some cases, ^{15}N fractionation is unknown, indicated by 'ε?'. Abbreviations: 2-OG, 2-oxoglutarate; 3PGA, 3-phosphoglycerate; Arg, arginine; Asp, aspartate; CBB cycle, Calvin-Benson-Bassham cycle; Gln, glutamine; Glu, glutamate; GOGAT, glutamate synthase; GS, glutamine synthetase; Gly, glycine; Met, methionine; Orn, ornithine; OAA, oxaloacetate; RuBP, ribulose bisphosphate;TCA cycle, tricarboxylic acid cycle; TP, triose-phosphate. Information compiled from multiple publications (Werner & Schmidt, 2002; Kroth et al., 2008; Tcherkez & Hodges, 2008; Smith et al., 2019)

Methionine $\delta^{15}N$ values in photosynthetic organisms are typically substantially lower than glutamate (Ishikawa *et al.*, 2018). Considering that aspartate $\delta^{15}N$ values are generally higher than those of glutamate (Tcherkez & Hodges, 2008), the relatively low methionine $\delta^{15}N$ values imply

strong ^{15}N fractionation during its synthesis or consumption. Diatoms possess a cobalamin (vitamin B_{12}) dependent methionine synthase enzyme MetH, and certain species also contain a cobalamin independent methionine synthase enzyme, MetE (Bertrand *et al.*, 2012). The latter is significantly less efficient compared to its cobalamin dependent counterpart. As such, during synthesis and processing of methionine, substantial changes in ^{15}N fractionation may occur depending on MetH or MetE utilization, which would be a reflection of vitamin B_{12} availability in the medium. Our batch cultures were setup with cobalamin concentrations substantially higher than in F/2 medium used in previous studies (Horn *et al.*, 2011; Robinson *et al.*, 2025), and it is therefore unlikely that vitamin B_{12} levels were low enough to influence methionine $\delta^{15}N$ values. Although an unlikely explanation of our results, the importance of methionine through its high contribution of N to polyamines and previously observed low $\delta^{15}N$ values (Ishikawa *et al.*, 2018), and the potential for vitamin B_{12} limited growth in oceans (Bertrand *et al.*, 2007), calls for experimental verification of this hypothesis.

An important input of N in the urea cycle is carbamoyl phosphate, formed from bicarbonate and ammonium (Fig. 8). The transcript of the enzyme for the synthesis of carbamoyl phosphate (unCPS) is more abundant under high light compared to low light (Bender *et al.*, 2012), indicating a sensitivity of N metabolism to light conditions. Moreover, unCPS transcript abundance was closely related to transcripts of glutamine synthesis in the chloroplast and mitochondrion, linking N-assimilation to the urea cycle. As opposed to higher plants where ammonium released from photorespiration and amino acid catabolism is predominantly re-assimilated in the chloroplast, in diatoms this ammonium can also be re-assimilated through synthesis of carbamoyl phosphate which is then processed in the urea cycle (Allen *et al.*, 2006, 2011; Parker *et al.*, 2008). Assuming that deamination reactions that release ammonium isotopically fractionate (Tcherkez & Hodges,

2008; Takizawa *et al.*, 2017), this pathway could shuttle N with distinct $\delta^{15}N$ values into the products of the urea cycle, which can then be redistributed to other amino acids.

Another notable result is the observed relationship between $\varepsilon_{biomass/NO3}$ values and the temporal change in $\varepsilon_{DB/biomass}$ over the course of batch culture progression (Fig. S4). During nitrate assimilation, nitrate is converted to nitrite and subsequently to ammonium. The conversion of nitrate to nitrite through nitrate reductase (NR) is typically the limiting step in this sequence. The magnitude of the associated ^{15}N fractionation, expressed as $\varepsilon_{biomass/NO3}$, depends on the balance between nitrate influx and efflux across the cell membrane (Granger *et al.*, 2010; Chen *et al.*, 2024). Hence, because $\varepsilon_{biomass/NO3}$ is largely governed by transport/diffusion and reduction kinetics, it is unlikely to directly cause the observed variation in $\varepsilon_{DB/biomass}$. Instead, the variable relationship between the two may reflect species-specific differences in N metabolism and the degree of internal N-isotope fractionation during biosynthetic processing of N. This interpretation is supported by the relation between amino acid $\delta^{15}N$ values and N-assimilation rates in higher plants (Tcherkez, 2010), and the connection between N-assimilation pathways and the urea cycle in diatoms (Bender *et al.*, 2012).

Ultimately, based on our experiments alone, it was not possible to reveal the exact mechanism by which $\varepsilon_{DB/biomass}$ has changed. Nevertheless, the results presented here strongly suggest sensitivity of frustule-bound $\delta^{15}N$ values to changes in growth conditions, such as light intensity and inorganic C availability, that affect metabolically driven ^{15}N fractionation during processing of organic N within the diatom cell. We thus hypothesize that alterations in metabolic fluxes in the N-assimilation, photorespiration and urea cycle pathways may play a particularly important role in ^{15}N fractionation of amino acids used for frustule-bound organic compound synthesis.

Implications and opportunities for the diatom frustule-bound nitrogen isotope paleo-proxy

The observed slower integration of nitrate $\delta^{15}N$ values into frustule-bound organic N compared to overall biomass is likely not important for paleorecords, as the timescale of this lag is very short (on the order of a few hours and possibly up to a few days) compared to the integration over multiple years to millenia in $\delta^{15}N_{DB}$ from sedimentary records. More importantly, for *A. granulata*, we showed that after this lag period, $\delta^{15}N_{DB}$ values follow those of biomass relatively closely (Fig. 7), confirming that, in theory, $\delta^{15}N_{DB}$ values are indeed faithfully tracking changes in nitrate $\delta^{15}N$ values over a wide range of $\delta^{15}N$ values.

Historically, $\delta^{15}N_{DB}$ values have been interpreted as a direct reflection of biomass $\delta^{15}N$ values. However, recent diatom culture studies, including the present work, have shown a concerning ambiguity in how closely $\delta^{15}N_{DB}$ values follow biomass $\delta^{15}N$ values (Horn *et al.*, 2011; Jones *et al.*, 2022; Robinson *et al.*, 2025). We hypothesize that there is growth condition and species-driven interaction between diatom C and N metabolism and ^{15}N fractionation leading to variation in $\delta^{15}N$ values of frustule-bound organic N that cannot be explained by biomass $\delta^{15}N$ values. Whether this interaction also impacts frustule-bound $\delta^{15}N$ values under growth conditions in the natural environment is not yet clear.

In sedimentary records from the Southern Ocean, diatom frustule-bound $\delta^{15}N$ has been shown to vary on glacial/interglacial timescales, with $\delta^{15}N_{DB}$ values up to 4 ‰ higher during glacial periods compared to interglacial periods (Robinson *et al.*, 2004; Studer *et al.*, 2015). Glacial/interglacial cycles are characterized by changes in atmospheric CO_2 concentrations and marine biological productivity, with lower atmospheric CO_2 and lower productivity in the Antarctic Ocean during ice ages compared to warm periods (Mortlock *et al.*, 1991; Petit *et al.*,

1999; Studer *et al.*, 2015). The increased glacial frustule-bound $\delta^{15}N$ values have mainly been attributed to reduced nitrate supply, leading to increased fractional nitrate consumption and thus higher $\delta^{15}N$ values incorporated into frustule-bound organic N (Robinson *et al.*, 2004; Studer *et al.*, 2015). In contrast to the natural environment, the batch culture experiments performed in our study represent near-unlimited nutrient conditions until nitrate concentrations approximate complete consumption. Despite this, $\varepsilon_{DB/biomass}$ was highly variable, implying that $\varepsilon_{DB/biomass}$ was likely not directly driven by the nutrient status of the medium, but rather by other factors, such as light conditions, inorganic C input, and/or cell density. Changes in the light conditions are likely not contributing to the changes in frustule-bound $\delta^{15}N$ values in paleorecords, since light-driven increased nitrate consumption would lead to increased productivity, which is in contrast to the observations from the Antarctic Ocean (Studer *et al.*, 2015). With respect to atmospheric CO_2 concentrations, it is important to consider whether diatom growth could have been C limited during ice ages, leading to the hypothesized changes in diatom metabolism in relation to internal biochemical ^{15}N fractionation. It is typically assumed that phytoplankton growth in the natural environment is not limited by inorganic C supply, but diatoms in particular can be limited by CO_2 availability during dense blooms, especially in air equilibrated surface ocean waters during glacial periods when atmospheric CO_2 concentrations were around 200 ppm (Riebesell *et al.*, 1993). Future experiments should verify whether the impact of C-limited growth on frustule-bound $\delta^{15}N$ values could be relevant for the observed frustule-bound $\delta^{15}N$ values from paleorecords. Overall, our results suggest that the signal generation of frustule-bound $\delta^{15}N$ values can be sensitive to growth conditions, which should be carefully considered in the interpretation of frustule-bound $\delta^{15}N$ values, especially in future diatom culture-based efforts to further ground-truth the frustule-bound $\delta^{15}N$ paleo proxy.

The continued development of the frustule-bound $\delta^{15}N$ paleo-proxy should aim to characterize the potential effects of diatom metabolism on frustule-bound $\delta^{15}N$ values. As discussed above, compound-specific ^{15}N-isotope analysis on biomass-derived amino acids will provide vital information linking diatom metabolism to isotopic fractionation that drives $\delta^{15}N_{DB}$. Additionally, once methods are available, $\delta^{15}N$ measurements of amino acids derived from the diatom frustule-bound organic N itself would be imperative for disentangling shifts in source-N $\delta^{15}N$ values, where all amino acid $\delta^{15}N$ values change similarly, and metabolically driven biochemical ^{15}N fractionation effects, where $\delta^{15}N$ values of amino acids would change relative to each other. Such methods have already been applied to mollusk shells from sediment records (Vokhshoori *et al.*, 2023) and its extended application to diatom frustules would be very valuable for the diatom frustule-bound $\delta^{15}N$ paleo proxy.

Conclusion

The results presented here show that biomass and frustule-bound $\delta^{15}N$ values can become decoupled in batch cultures, and that this decoupling cannot be explained by differences in isotopic integration timing. We find that $\delta^{15}N_{DB}$ is indeed driven by $\delta^{15}N$ values of assimilated nitrate in ^{15}N-labeled nitrate experiments, but under natural abundance conditions, the ^{15}N fractionation during processing of organic N in the cell substantially influences $\delta^{15}N_{DB}$. We hypothesize that this offset arises from growth condition-dependent shift in metabolic fluxes, which influence ^{15}N fractionation during amino acid synthesis and the formation of frustule-bound organic compounds. Future ground-truthing efforts should aim to quantify the extent and drivers of decoupling between bulk-biomass and frustule-bound $\delta^{15}N$ under controlled, multi-factorial environmental conditions. Such experiments would improve our understanding of how $\delta^{15}N_{DB}$ values respond to physiological variation during diatom growth, ultimately enhancing the reliability of the $\delta^{15}N_{DB}$

paleo-proxy for reconstructing N cycling and changing environmental conditions in aquatic systems over large time scales.

Acknowledgements

Funding for this study was provided by Swiss National Science Foundation grant 200021_200766 to A.S.S. and by resources provided by the University of Basel. We would like to thank Marta Reyes (EAWAG) for providing freshwater diatom cultures and help with diatom culturing techniques; Thomas Kuhn (Uni. Basel) for help with Flash-EA IRMS analyses of biomass samples and general help in the lab; Klaus Schläppi (Uni. Basel) for providing the SANYO climate chambers; Gregory de Souza (ETH Zürich) for help with silicate concentration analysis; Guillaume Tcherkez (Uni. Angers), Roland Werner (ETH Zürich) and Peter Kroth (Uni. Konstanz) for helpful discussion of biochemical ^{15}N fractionation and diatom metabolism.

References

Admiraal W, Peletier H, Laane RWPM. **1986**. Nitrogen metabolism of marine planktonic diatoms; excretion, assimilation and cellular pools of free amino acids in seven species with different cell size. *Journal of Experimental Marine Biology and Ecology* **98**: 241–263.

Ai XE, Studer AS, Sigman DM, Martínez-García A, Fripiat F, Thöle LM, Michel E, Gottschalk J, Arnold L, Moretti S, *et al.* 2020. Southern Ocean upwelling, Earth's obliquity, and glacial-interglacial atmospheric CO_2 change. *Science* **370**: 1348–1352.

Allen AE, Dupont CL, Oborník M, Horák A, Nunes-Nesi A, McCrow JP, Zheng H, Johnson DA, Hu H, Fernie AR, *et al.* 2011. Evolution and metabolic significance of the urea cycle in photosynthetic diatoms. *Nature* **473**: 203–207.

Allen AE, Vardi A, Bowler C. **2006**. An ecological and evolutionary context for integrated nitrogen metabolism and related signaling pathways in marine diatoms. *Current Opinion in Plant Biology* **9**: 264–273.

Bender SJ, Parker MS, Armbrust EV. **2012**. Coupled Effects of Light and Nitrogen Source on the Urea Cycle and Nitrogen Metabolism over a Diel Cycle in the Marine Diatom *Thalassiosira pseudonana*. *Protist* **163**: 232–251.

Berges JA, Franklin DJ, Harrison PJ. **2001**. Evolution of an Artificial Seawater Medium: Improvements in Enriched Seawater, Artificial Water Over the Last Two Decades. *Journal of Phycology* **37**: 1138–1145.

Bertrand EM, Allen AE, Dupont CL, Norden-Krichmar TM, Bai J, Valas RE, Saito MA. **2012**. Influence of cobalamin scarcity on diatom molecular physiology and identification of a cobalamin acquisition protein. *Proceedings of the National Academy of Sciences* **109**: E1762–E1771.

Bertrand EM, Saito MA, Rose JM, Riesselman CR, Lohan MC, Noble AE, Lee PA, DiTullio GR. **2007**. Vitamin B12 and iron colimitation of phytoplankton growth in the Ross Sea. *Limnology and Oceanography* **52**: 1079–1093.

Braman RS, Hendrix SA. **1989**. Nanogram nitrite and nitrate determination in environmental and biological materials by vanadium (III) reduction with chemiluminescence detection. *Analytical Chemistry* **61**: 2715–2718.

Bridoux MC, Ingalls AE. **2010**. Structural identification of long-chain polyamines associated with diatom biosilica in a Southern Ocean sediment core. *Geochimica et Cosmochimica Acta* **74**: 4044–4057.

Bridoux MC, Keil RG, Ingalls AE. **2012**. Analysis of natural diatom communities reveals novel insights into the diversity of long chain polyamine (LCPA) structures involved in silica precipitation. *Organic Geochemistry* **47**: 9–21.

Brunelle BG, Sigman DM, Cook MS, Keigwin LD, Haug GH, Plessen B, Schettler G, Jaccard SL. **2007**. Evidence from diatom-bound nitrogen isotopes for subarctic Pacific stratification during the last ice age and a link to North Pacific denitrification changes. *Paleoceanography* **22**.

Burkhardt S, Riebesell U, Zondervan I. **1999**. Stable carbon isotope fractionation by marine phytoplankton in response to daylength, growth rate, and CO_2 availability. *Marine Ecology Progress Series* **184**: 31–41.

Chen Y, Yang JT, Tang J, Hong H, Kao S, Dai M, Shi D. **2024**. Changes in isotope fractionation during nitrate assimilation by marine eukaryotic and prokaryotic algae under different pH and CO_2 conditions. *Limnology and Oceanography* **69**: 1045–1055.

Clement R, Dimnet L, Maberly SC, Gontero B. **2016**. The nature of the CO_2 -concentrating mechanisms in a marine diatom, *Thalassiosira pseudonana*. *New Phytologist* **209**: 1417–1427.

Conley DJ, Kilham SS, Theriot E. **1989**. Differences in silica content between marine and freshwater diatoms. *Limnology and Oceanography* **34**: 205–212.

Coplen TB. **2011**. Guidelines and recommended terms for expression of stable-isotope-ratio and gas-ratio measurement results. *Rapid Communications in Mass Spectrometry* **25**: 2538–2560.

Degens ET, Guillard RRL, Sackett WM, Hellebust JA. **1968**. Metabolic fractionation of carbon isotopes in marine plankton—I. Temperature and respiration experiments. *Deep Sea Research and Oceanographic Abstracts* **15**: 1–9.

Deuser WG. **1970**. Isotopic Evidence for Diminishing Supply of Available Carbon during Diatom Bloom in the Black Sea. *Nature* **225**: 1069–1071.

Dove IA, Bishop IW, Crosta X, Riedinger N, Kelly RP, Robinson RS. **2025**. *Chaetoceros* Resting Spores Do Not Significantly Bias Sedimentary Diatom-Bound Nitrogen Isotope Records Despite Distinctly Low Values. *Paleoceanography and Paleoclimatology* **40**: e2024PA005041.

Fry B. **1996**. $^{13}C/^{12}C$ fractionation by marine diatoms. *Marine Ecology Progress Series* **134**: 283–294.

Gauthier PPG, Lamothe M, Mahé A, Molero G, Nogués S, Hodges M, Tcherkez G. **2013**. Metabolic origin of $\delta^{15}N$ values in nitrogenous compounds from Brassica napus L. leaves. *Plant, Cell & Environment* **36**: 128–137.

Granger J, Sigman DM, Rohde MM, Maldonado MT, Tortell PD. **2010**. N and O isotope effects during nitrate assimilation by unicellular prokaryotic and eukaryotic plankton cultures. *Geochimica et Cosmochimica Acta* **74**: 1030–1040.

Guy RD, Vanlerberghe GC, Turpin DH. **1989**. Significance of Phosphoenolpyruvate Carboxylase during Ammonium Assimilation: Carbon Isotope Discrimination in Photosynthesis and Respiration by the N-Limited Green Alga *Selenastrum minutum*. *Plant Physiology* **89**: 1150–1157.

Harrison PJ, Waters RE, Taylor FJR. **1980**. A Broad Spectrum Artificial Sea Water Medium for Coastal and Open Ocean Phytoplankton. *Journal of Phycology* **16**: 28–35.

Horn MG, Robinson RS, Rynearson TA, Sigman DM. **2011**. Nitrogen isotopic relationship between diatom-bound and bulk organic matter of cultured polar diatoms. *Paleoceanography* **26**: 2010PA002080.

Ishikawa NF, Chikaraishi Y, Takano Y, Sasaki Y, Takizawa Y, Tsuchiya M, Tayasu I, Nagata T, Ohkouchi N. **2018**. A new analytical method for determination of the nitrogen isotopic composition of methionine: Its application to aquatic ecosystems with mixed resources. *Limnology and Oceanography: Methods* **16**: 607–620.

Jones CA, Closset I, Riesselman CR, Kelly RP, Brzezinski MA, Robinson RS. **2022**. New Constraints on Assemblage-Driven Variation in the Relationship Amongst Diatom-Bound, Biomass, and Nitrate Nitrogen Isotope Values. *Paleoceanography and Paleoclimatology* **37**: e2022PA004428.

Kalansky JF, Robinson RS, Popp BN. **2011**. Insights into nitrogen cycling in the western Gulf of California from the nitrogen isotopic composition of diatom-bound organic matter. *Geochemistry, Geophysics, Geosystems* **12**.

Kirkham AR, Richthammer P, Schmidt K, Wustmann M, Maeda Y, Hedrich R, Brunner E, Tanaka T, van Pée K-H, Falciatore A, *et al.* 2017. A role for the cell-wall protein silacidin in cell size of the diatom *Thalassiosira pseudonana*. *The ISME Journal* **11**: 2452–2464.

Kotzsch A, Gröger P, Pawolski D, Bomans PHH, Sommerdijk NAJM, Schlierf M, Kröger N. **2017**. Silicanin-1 is a conserved diatom membrane protein involved in silica biomineralization. *BMC Biology* **15**: 65.

Kröger N, Poulsen N. **2008**. Diatoms—From Cell Wall Biogenesis to Nanotechnology. *Annual Review of Genetics* **42**: 83–107.

Kroth PG, Chiovitti A, Gruber A, Martin-Jezequel V, Mock T, Parker MS, Stanley MS, Kaplan A, Caron L, Weber T, *et al.* 2008. A Model for Carbohydrate Metabolism in the Diatom *Phaeodactylum tricornutum* Deduced from Comparative Whole Genome Analysis. *PLOS ONE* **3**: e1426.

Kudo I. **2003**. Change in the uptake and cellular Si:N ratio in diatoms responding to the ambient Si:N ratio and growth phase. *Marine Biology* **143**: 39–46.

Lehmann MF, Bernasconi SM, Barbieri A, McKenzie JA. **2002**. Preservation of organic matter and alteration of its carbon and nitrogen isotope composition during simulated and in situ early sedimentary diagenesis. *Geochimica et Cosmochimica Acta* **66**: 3573–3584.

Lin H-Y, Liu C-H, Kang Y-T, Lin S-W, Liu H-Y, Lee C-T, Liu Y-C, Hsu M-C, Chien Y-Y, Hong S-M, *et al.* 2024. Enhancing the Spermidine Synthase-Based Polyamine Biosynthetic Pathway to Boost Rapid Growth in Marine Diatom Phaeodactylum tricornutum. *Biomolecules* **14**: 372.

Macko SA, Fogel ML, Hare PE, Hoering TC. **1987**. Isotopic fractionation of nitrogen and carbon in the synthesis of amino acids by microorganisms. *Chemical Geology: Isotope Geoscience section* **65**: 79–92.

Mariotti A, Germon JC, Hubert P, Kaiser P, Letolle R, Tardieux A, Tardieux P. **1981**. Experimental determination of nitrogen kinetic isotope fractionation: Some principles; illustration for the denitrification and nitrification processes. *Plant and Soil* **62**: 413–430.

McCarthy MD, Lehman J, Kudela R. **2013**. Compound-specific amino acid δ^{15}N patterns in marine algae: Tracer potential for cyanobacterial vs. eukaryotic organic nitrogen sources in the ocean. *Geochimica et Cosmochimica Acta* **103**: 104–120.

McMahon KW, McCarthy MD. **2016**. Embracing variability in amino acid δ¹⁵N fractionation: mechanisms, implications, and applications for trophic ecology. *Ecosphere* **7**: e01511.

Morales LV, Granger J, Chang BX, Prokopenko MG, Plessen B, Gradinger R, Sigman DM. **2014**. Elevated ^{15}N/^{14}N in particulate organic matter, zooplankton, and diatom frustule-bound nitrogen in the ice-covered water column of the Bering Sea eastern shelf. *Deep Sea Research Part II: Topical Studies in Oceanography* **109**: 100–111.

Morales LV, Sigman DM, Horn MG, Robinson RS. **2013**. Cleaning methods for the isotopic determination of diatom-bound nitrogen in non-fossil diatom frustules. *Limnology and Oceanography: Methods* **11**: 101–112.

Mortlock RA, Charles CD, Froelich PN, Zibello MA, Saltzman J, Hays JD, Burckle LH. **1991**. Evidence for lower productivity in the Antarctic Ocean during the last glaciation. *Nature* **351**: 220–223.

Needoba JA, Waser NA, Harrison PJ, Calvert SE. **2003**. Nitrogen isotope fractionation in 12 species of marine phytoplankton during growth on nitrate. *Marine Ecology Progress Series* **255**: 81–91.

Parker MS, Armbrust EV, Piovia-Scott J, Keil RG. **2004**. Induction of Photorespiration by Light in the Centric Diatom *Thalassiosira weissflogii* (bacillariophyceae): Molecular Characterization and Physiological Consequences. *Journal of Phycology* **40**: 557–567.

Parker MS, Mock T, Armbrust EV. **2008**. Genomic Insights into Marine Microalgae. *Annual Review of Genetics* **42**: 619–645.

Petit JR, Jouzel J, Raynaud D, Barkov NI, Barnola J-M, Basile I, Bender M, Chappellaz J, Davis M, Delaygue G, *et al.* 1999. Climate and atmospheric history of the past 420,000 years from the Vostok ice core, Antarctica. *Nature* **399**: 429–436.

Poulsen N, Sumper M, Kröger N. **2003**. Biosilica formation in diatoms: Characterization of native silaffin-2 and its role in silica morphogenesis. *Proceedings of the National Academy of Sciences* **100**: 12075–12080.

R Core Team. **2023**. R: A language and environment for statistical computing.

Racusen D, Foote M. **1960**. Amino acid turnover and protein synthesis in leaves. *Archives of Biochemistry and Biophysics* **90**: 90–95.

Richthammer P, Börmel M, Brunner E, van Pée K-H. **2011**. Biomineralization in Diatoms: The Role of Silacidins. *ChemBioChem* **12**: 1362–1366.

Riebesell U, Wolf-Gladrow DA, Smetacek V. **1993**. Carbon dioxide limitation of marine phytoplankton growth rates. *Nature* **361**: 249–251.

Robinson RS, Brunelle BG, Sigman DM. **2004**. Revisiting nutrient utilization in the glacial Antarctic: Evidence from a new method for diatom-bound N isotopic analysis. *Paleoceanography* **19**.

Robinson RS, Jones CA, Dove IA, Kelly RP, Brzezinski MA. **2025**. Monospecific Diatom Cultures Suggest Potential Interspecies Variation of Diatom-Bound Nitrogen Isotope Signatures Associated With Silica Acquisition. *Geochemistry, Geophysics, Geosystems* **26**: e2024GC011923.

Robinson RS, Jones CA, Kelly RP, Love A, Closset I, Rafter PA, Brzezinski M. **2020**. A Test of the Diatom-Bound Paleoproxy: Tracing the Isotopic Composition of Nutrient-Nitrogen Into Southern Ocean Particles and Sediments. *Global Biogeochemical Cycles* **34**: e2019GB006508.

Robinson RS, Kienast M, Luiza Albuquerque A, Altabet M, Contreras S, De Pol Holz R, Dubois N, Francois R, Galbraith E, Hsu T-C, *et al.* 2012. A review of nitrogen isotopic alteration in marine sediments. *Paleoceanography* **27**.

Robinson DB, Rognlien JL, Bauer CA, Simmons BA. **2007**. Dependence of amine-accelerated silicate condensation on amine structure. *Journal of Materials Chemistry* **17**: 2113.

Robinson RS, Sigman DM, DiFiore PJ, Rohde MM, Mashiotta TA, Lea DW. **2005**. Diatom-bound $^{15}N/^{14}N$: New support for enhanced nutrient consumption in the ice age subantarctic. *Paleoceanography* **20**.

Sharkey TD, Berry JA. **1985**. Carbon isotope fractionation of algae as influenced by an inducible CO_2 concentrating mechanism. *Inorganic carbon uptake by aquatic photosynthetic organisms*: 389–401.

Sigman DM, Altabet MA, Francois R, McCorkle DC, Gaillard J-F. **1999**. The isotopic composition of diatom-bound nitrogen in Southern Ocean sediments. *Paleoceanography* **14**: 118–134.

Sigman DM, Casciotti KL, Andreani M, Barford C, Galanter M, Böhlke JK. **2001**. A Bacterial Method for the Nitrogen Isotopic Analysis of Nitrate in Seawater and Freshwater. *Analytical Chemistry* **73**: 4145–4153.

Smith SR, Dupont CL, McCarthy JK, Broddrick JT, Oborník M, Horák A, Füssy Z, Cihlář J, Kleessen S, Zheng H, *et al.* 2019. Evolution and regulation of nitrogen flux through compartmentalized metabolic networks in a marine diatom. *Nature Communications* **10**: 4552.

Stief P, Schauberger C, Lund MB, Greve A, Abed RMM, Al-Najjar MAA, Attard K, Bonaglia S, Deutzmann JS, Franco-Cisterna B, *et al.* 2022. Intracellular nitrate storage by diatoms can be an important nitrogen pool in freshwater and marine ecosystems. *Communications Earth & Environment* **3**: 154.

Strickland JDH, Parsons TR. **1972**. A Practical Handbook of Seawater Analysis, 2nd edition.

Studer AS, Sigman DM, Martínez-García A, Benz V, Winckler G, Kuhn G, Esper O, Lamy F, Jaccard SL, Wacker L, *et al.* 2015. Antarctic Zone nutrient conditions during the last two glacial cycles. *Paleoceanography* **30**: 845–862.

Studer AS, Wörmer L, Vogel H, Dubois N, Bartosiewicz M, Hinrichs K-U, Lepori F, Lehmann MF. **2024**. First lacustrine application of the diatom-bound nitrogen isotope paleo-proxy reveals coupling of denitrification and N fixation in a hyper-eutrophic lake. *Limnology and Oceanography* **69**: 1797–1809.

Sumper M, Brunner E. **2008**. Silica Biomineralisation in Diatoms: The Model Organism Thalassiosira pseudonana. *ChemBioChem* **9**: 1187–1194.

Takizawa Y, Dharampal PS, Steffan SA, Takano Y, Ohkouchi N, Chikaraishi Y. **2017**. Intra-trophic isotopic discrimination of $^{15}N/^{14}N$ for amino acids in autotrophs: Implications for nitrogen dynamics in ecological studies. *Ecology and Evolution* **7**: 2916–2924.

Tcherkez G. **2010**. Natural $^{15}N/^{14}N$ isotope composition in C_3 leaves: are enzymatic isotope effects informative for predicting the 15N-abundance in key metabolites? *Functional Plant Biology* **38**: 1–12.

Tcherkez G, Hodges M. **2008**. How stable isotopes may help to elucidate primary nitrogen metabolism and its interaction with (photo)respiration in C_3 leaves. *Journal of Experimental Botany* **59**: 1685–1693.

Tesson B, Lerch SJL, Hildebrand M. **2017**. Characterization of a New Protein Family Associated With the Silica Deposition Vesicle Membrane Enables Genetic Manipulation of Diatom Silica. *Scientific Reports* **7**: 13457.

Tortell PD. **2000**. Evolutionary and ecological perspectives on carbon acquisition in phytoplankton. *Limnology and Oceanography* **45**: 744–750.

Vokhshoori NL, Rick TC, Braje TJ, McCarthy MD. **2023**. Preservation of stable isotope signatures of amino acids in diagenetically altered Middle to Late Holocene archaeological mollusc shells. *Geochimica et Cosmochimica Acta* **352**: 36–50.

Waser NAD, Harrison PJ, Nielsen B, Calvert SE, Turpin DH. **1998**. Nitrogen isotope fractionation during the uptake and assimilation of nitrate, nitrite, ammonium, and urea by a marine diatom. *Limnology and Oceanography* **43**: 215–224.

Werner RA, Schmidt H-L. **2002**. The in vivo nitrogen isotope discrimination among organic plant compounds. *Phytochemistry* **61**: 465–484.

Yoneyama T, Fujihara S, Yagi K. **1998**. Natural abundance of ^{15}N in amino acids and polyamines from leguminous nodules: unique ^{15}N enrichment in homospermidine. *Journal of Experimental Botany* **49**: 521–526.